Computer Modeling in Engineering & Sciences

Tech Science Press

https://doi.org/10.32604/cmes.2026.086187 Published Online: 30 October 2026

ARTICLE

System Identification of Infinite Impulse Response Filters through a Novel Hybrid Starfish–Differential Evolution Optimization Method

Serdar Ekinci[1], Ridvan Firat Cinar[2], Davut Izci[3,*], Gökhan Yüksek[4], Vedat Tümen[1], Timur Lale[4], Behçet Kocaman[5], Filiz Karaomerlioglu[6], Fahmi Elsayed[7] and Mohammad Salman[7]

[1]Department of Computer Engineering, Bitlis Eren University, Bitlis, Turkey
[2]Department of Computer Engineering, Batman University, Batman, Turkey
[3]Department of Electrical and Electronic Engineering, Bursa Uludag University, Bursa, Turkey
[4]Department of Electrical and Electronics Engineering, Batman University, Batman, Turkey
[5]Department of Electrical and Electronics Engineering, Bitlis Eren University, Bitlis, Turkey
[6]Department of Electrical and Electronics Engineering, Mersin University, Ciftlikkoy, Mersin, Turkey
[7]College of Engineering and Technology, American University of the Middle East, Egaila 54200, Kuwait

*Corresponding Author: Davut Izci. Email: davutizci@uludag.edu.tr

Received: 26 May 2026; Accepted: 08 October 2026

ABSTRACT: Identifying the parameters of infinite impulse response (IIR) filters is a challenging optimization problem due to the nonlinear and multimodal structure of the error surface, together with stability constraints. Existing metaheuristic methods often exhibit premature convergence or insufficient refinement in later stages, limiting estimation accuracy. This paper proposes the hybrid starfish–differential evolution optimization algorithm (HSFOADE), which integrates difference-based mutation and greedy selection into the starfish optimization framework. This design combines stochastic exploration with controlled directional refinement, enabling more stable updates during the search process. The proposed method is evaluated on second- and fifth-order IIR systems under both same-order and reduced-order identification scenarios. Comparative results against several baseline and recent methods show lower estimation error, faster convergence, and reduced parameter variance. The findings indicate that the proposed mechanism improves search stability and estimation consistency without increasing computational complexity.

KEYWORDS: Starfish optimization algorithm; mutation and crossover strategies; differential evolution; infinite impulse response; system identification

1 Introduction

1.1 Related Work and Research Gap

The pursuit of optimized digital filters has always been closely tied to the history of signal processing itself. From the earliest days of telecommunication to the current age of wireless networks, engineers have sought mathematical structures capable of shaping signals with precision while using minimal computational resources [1–3]. Analytical frameworks provided early successes, giving rise to systematic methods for designing canonical filters. Over time, however, the growing complexity of applications, from adaptive antennas in modern 6G systems to wearable biomedical devices monitoring human physiology, demanded solutions that extended beyond fixed formulas and static design charts [4–6]. This demand gradually opened the door to the idea that optimization itself could be inspired by natural or biological processes [7,8],

Copyright © 2026 The Authors. Published by Tech Science Press. This work is licensed under a Creative Commons Attribution 4.0 International License, which permits unrestricted use, distribution, and reproduction in any medium, provided the original work is properly cited.

yielding strategies that were more flexible, adaptive, and able to search through complex design spaces where traditional mathematics struggled.

Within this broader landscape, infinite impulse response (IIR) [9,10] filters have held a central and persistent importance. Their ability to approximate desired frequency responses with significantly fewer coefficients than finite impulse response (FIR) filters makes them uniquely attractive when compactness and efficiency are essential. Communication systems rely on IIR structures for equalization and channel shaping; control systems use them to embed dynamics in real time; audio and radar technologies depend on them for extracting meaningful information from noisy or rapidly changing signals; and biomedical devices favour their low-order implementation to balance accuracy with strict power and hardware constraints [11–14]. This breadth of applications underscores the enduring role of IIR filters in bridging mathematical elegance with engineering necessity. However, designing these filters is far from trivial. Unlike their FIR counterparts, IIR structures involve recursive feedback, and this recursive nature places stability at the heart of the design challenge. A well-chosen set of coefficients produces compact and reliable performance, but a poorly tuned denominator term can push poles outside the unit circle, destabilizing the entire system. Compounding this difficulty is the nature of the optimization surface: highly nonlinear, multimodal, and riddled with local minima.

Traditional solutions, such as Butterworth, Chebyshev, and elliptic filter designs, emerged as systematic attempts to address these issues [15–17]. Each of these families offers distinctive trade-offs between passband flatness, transition sharpness, and stopband attenuation, and they are supported by decades of theoretical refinement. They remain essential tools in the signal processing toolkit, often serving as the first approach taught to students and applied in practice. However, their utility begins to fade when real-world conditions impose more demanding constraints, multiple frequency bands that require simultaneous shaping, adaptive scenarios where parameters must change on the fly, or high-order systems that amplify numerical sensitivity. In such situations, the classical designs no longer guarantee satisfactory solutions, producing suboptimal filters or failing to enforce stability while minimizing error. This growing mismatch between application requirements and available classical methods reveals a fundamental gap: the need for optimization strategies that can traverse complex, nonconvex search spaces without becoming trapped in local optima.

Metaheuristic approaches for IIR filter design and system identification can be broadly categorized into nature-inspired, physics-inspired, and hybrid frameworks. Nature-inspired methods include genetic algorithm (GA) [18], particle swarm optimization (PSO) [19,20], differential evolution (DE) [21,22], grey wolf optimizer (GWO) [23], artificial bee colony (ABC) [24], dragonfly algorithm (DA) [25], firefly algorithm (FA) [26,27], cat swarm optimization (CSO) [28], enzyme action optimizer (EAO) [29,30], hippopotamus algorithm [31], and more recent designs such as artificial hummingbird optimizer (AHO) [32,33], artificial rabbits optimization (ARO) [34], lotus effect optimisation algorithm (LEA) [35], social network optimization algorithm via centrality and influence-based learning (SOCIAL) [36] and starfish optimization algorithm (SFOA) [37]. Physics-inspired algorithms such as gravitational search algorithm (GSA) [38], water wave optimization (WWO) [39], and inclined planes system optimization (IPSO) [40] have also been employed for IIR identification, exploiting simplified analogies to natural physical processes. In addition, hybrid or ensemble strategies have been proposed to overcome limitations of single algorithms, including hybrid optimization technique based on the combination of cellular particle swarm optimization and differential evolution (CPSO–DE) [41], seeker optimization algorithm (SOA) [42], memetic approaches [43], moth flame optimization with variable neighbourhood search (MFO-VNS) [44], and hybridization of gazelle optimizer with simulated annealing (GOA-SA) [45]. Beyond these representative cases, the literature also includes a broad range of enhanced and problem-specific metaheuristics. Improved evolutionary and swarm-based methods have been proposed, such as immune-inspired variants [46], teaching–learning-based optimization

(TLBO) [47], sparrow search algorithm [48], hunger games pattern search [49], each aiming to refine global exploration and prevent premature convergence. Hybrid designs extend this trend by integrating multiple strategies into a single framework, for instance pattern search–enhanced arithmetic optimization (PS-AOA) [50], modified artificial bee colony algorithms [51], or the improved cooperation search optimization algorithm [52], weighted sum–variable length particle swarm optimization [53], logarithmic spiral based artificial bee colony (Ls-ABC) [54], adaptive multiple-elites-guided composite differential evolution algorithm (AMECoDEs) [55]. Hardware-oriented hybrids, such as artificial rabbits optimization adapted for (field-programmable gate array) FPGA implementation [56–58], further highlight the growing attention to practical deployment.

A number of specialized or adaptive frameworks have been developed to address reduced-order and complex modelling cases. Examples include manta ray foraging optimization (MRFO) for reduced-order modelling [59], fractional-order designs with mayfly optimization [60], and artificial intelligence optimization methods [61]. More recent contributions involve gbest-guided atom search optimization (mASA) [62], atom search optimization (ASO) [63], chaotic oppositional-based whale optimization algorithm (COWOA) [64], and ecosystem-inspired hybrids with opposition-based learning [65,66]. Collectively, these studies demonstrate the richness of metaheuristic adaptations to IIR filter design, while at the same time reinforcing a common observation: although each method contributes specific improvements, challenges such as local stagnation, sensitivity in denominator estimation, and balancing accuracy with model compactness remain unresolved, leaving room for novel hybrid strategies like hybrid starfish–differential evolution optimization.

To address these long-standing challenges, researchers have increasingly turned toward hybrid and improved metaheuristic designs. The underlying idea is that no single strategy is universally effective, but by combining complementary mechanisms, it becomes possible to achieve a better balance between global exploration and local refinement. Memetic algorithms, for instance, enrich global search with problem-specific local adjustments, enabling the optimizer to escape shallow minima while fine-tuning promising regions. Selective mechanism-based strategies introduce adaptive rules that switch between operators depending on the search stage, improving convergence dynamics over purely random exploration. Similarly, combinations of classical population-based optimizers with deterministic local search methods provide a layered approach: the stochastic component explores the broader space. In contrast, the deterministic step sharpens accuracy near candidate optima.

Despite these advancements, the design of IIR filters continues to pose difficulties. When the system order increases, the parameter space expands exponentially, making premature convergence and instability more likely. Even algorithms equipped with hybrid operators can falter in ensuring precise denominator estimation, which is essential to maintaining system stability. Reduced-order modelling further complicates matters, since the intentional mismatch between the model and the proper system introduces approximation errors that interact with the optimization process. This dual challenge requires not only minimizing the error between outputs but also preserving dominant system dynamics in a compact form. In practice, this means that the optimizer must simultaneously balance two conflicting goals: achieving high accuracy while enforcing simplicity and stability. The persistence of these problems has motivated the exploration of new algorithmic designs that can sustain both efficiency and accuracy across a broader range of identification scenarios.

Against this backdrop, a new generation of bio-inspired algorithms has attracted significant attention for their ability to strike a more effective balance between exploration and exploitation. Among them, SFOA stands out as a recent contribution, drawing inspiration from three principal starfish behaviours: exploration, preying, and regeneration [37]. These behaviours are translated into exploration, preying, and

regeneration mechanisms that support global search and population diversity. Through these mechanisms, SFOA has demonstrated competitive performance across diverse benchmark problems and engineering optimization tasks, often surpassing more established metaheuristics in terms of global search capacity. Nevertheless, when applied to the intricate domain of IIR filter identification, the algorithm still reveals certain shortcomings. In particular, it may stagnate around local minima during high-dimensional searches and struggles to provide precise refinement of denominator coefficients, which are critical for ensuring system stability. This tension between strong exploration and limited fine-tuning highlights the need for further enhancement of the SFOA framework. Recent studies have also proposed several enhanced SFOA-based variants for general optimization and engineering design problems [67,68]. These studies indicate that the original SFOA framework has attracted increasing attention and that its exploration–exploitation structure can be further improved through additional search strategies. However, these variants are mainly developed for general-purpose benchmark optimization, whereas the present study focuses on embedding difference-based refinement into SFOA for stability-sensitive IIR system identification.

These shortcomings motivate the incorporation of complementary operators that can strengthen both diversity and precision in the search process. DE is well suited for this purpose because its mutation and crossover operators introduce difference-based variation and directional refinement during the search process. By embedding these DE operators into the SFOA framework, a hybrid algorithm referred to as HSFOADE is established. This integration preserves the exploratory strength of SFOA, ensuring that the search can still cover a vast solution space, while simultaneously enhancing its exploitation capacity through DE-driven updates that refine candidate solutions with greater accuracy. As a result, HSFOADE is expected to converge more rapidly, achieve lower error levels, and deliver more accurate coefficient estimation. Significantly, the hybridization also improves the ability to maintain stable denominator parameters, a critical requirement in IIR filter identification where pole locations directly determine system stability. Through this combination, HSFOADE provides a more balanced and reliable optimization pathway for addressing the inherent challenges of IIR modelling.

The practical importance of such improvements extends to multiple domains. In communication systems, adaptive IIR filters are employed for tasks such as channel equalization and spectrum shaping, where stability monitoring during coefficient adaptation is essential [69]. In control engineering, accurate identification enables effective controller design and stability assurance [70–73]. Biomedical signal processing benefits from compact recursive filters that can be executed in real time on low-power embedded hardware [74]. Applications in radar and audio systems also rely heavily on efficient IIR structures for real-time implementation [75,76]. HSFOADE directly addresses these needs by providing more accurate approximations with manageable computational cost, making it suitable for practical deployments.

1.2 Research Gap Analysis

Despite the extensive development of metaheuristic algorithms for IIR system identification, a consistent limitation emerges across different algorithmic families. Population-based methods such as PSO and GWO provide efficient global exploration but often suffer from premature convergence and insufficient fine-tuning of denominator coefficients. DE offers strong directional variation and exploitation capability; however, it may lose diversity in later stages and struggle to maintain stability-sensitive parameter balance. Recent algorithms such as SFOA improve exploration through stochastic and regeneration-based mechanisms, yet they lack structured directional refinement, which is essential for precise coefficient estimation in multimodal error surfaces.

These observations reveal a clear research gap: the absence of a unified optimization framework that simultaneously preserves population diversity while enabling controlled, difference-based refinement.

The proposed HSFOADE is designed to address this gap by integrating stochastic exploration dynamics with differential mutation and greedy selection, thereby achieving a balanced and adaptive search process evaluated for the requirements of IIR system identification.

To formalize this observation, a structured comparison of representative metaheuristic algorithms is provided in Table 1, where their exploration capability, exploitation behaviour, and inherent limitations in stability-sensitive parameter estimation are systematically summarized. As observed from Table 1, no single algorithm simultaneously ensures strong population diversity and controlled directional refinement, which reveals a critical gap in existing optimization frameworks. This gap becomes particularly significant in IIR system identification, where accurate estimation of denominator coefficients requires both global exploration and stable local refinement.

Table 1: Comparative strengths and limitations of representative metaheuristic algorithms for IIR system identification.

Method	Strength	Limitation
PSO/GWO	Fast convergence, efficient global search	Premature convergence, weak fine-tuning
DE	Directional variation, strong exploitation	Diversity loss in later stages
SFOA	Strong exploration, population diversity	Lack of directional refinement
HSFOADE (proposed)	Balanced exploration–exploitation, stable convergence	—

1.3 Motivation, Novelty and Algorithmic Justification

The motivation of this study arises from the need to overcome the imbalance between exploration and directional refinement observed in existing metaheuristic algorithms for IIR system identification. Despite the promising exploration capability of SFOA, its position update mechanism relies primarily on stochastic trigonometric perturbations and distance-based attraction, which may limit directional refinement in high-dimensional and multimodal error surfaces. This limitation becomes critical in IIR system identification, where precise estimation of denominator coefficients directly governs system stability.

To address this issue, DE operators are incorporated to introduce structured, difference-based variation and greedy selection into the search process. This modification transforms the update dynamics from predominantly stochastic exploration into a hybrid mechanism that combines population diversity with directional refinement. Unlike standard hybrid approaches, this integration specifically targets variance reduction in promising regions while preserving global search capability, resulting in improved convergence behaviour and more accurate parameter estimation. This integration is therefore not a simple hybridization, but a mechanism-driven modification of the search dynamics.

As a direct consequence of this mechanism, the novelty of this work lies in the introduction of HSFOADE as a new hybrid optimizer introduced and evaluated for IIR system identification. Unlike conventional SFOA or DE when applied individually, the hybrid approach achieves consistently lower error levels, faster convergence, and tighter parameter distributions. Comparative analysis against both baseline algorithms and advanced methods reported in the literature demonstrates that HSFOADE delivers measurable performance gains. The contributions of this study, therefore, include the development of the hybrid method, the demonstration of its effectiveness on both same-order and reduced-order IIR systems, and the validation of its applicability in nonlinear engineering contexts. The study also extends the validation beyond IIR system identification by including selected CEC2022 (Congress on Evolutionary

Computation 2022) benchmark functions, allowing the proposed HSFOADE mechanism to be assessed in a broader numerical optimization context.

It should be emphasized that the contribution of the proposed HSFOADE framework does not arise from hybridization alone. The novelty lies in the sequential embedded interaction established between DE-based refinement and SFOA population dynamics within a unified iterative structure. In the proposed mechanism, DE mutation and crossover are applied as an embedded refinement stage before the SFOA exploration–exploitation update, enabling difference-based directional information to influence the subsequent population evolution. This interaction modifies the update behaviour of the original SFOA by combining stochastic exploration and regeneration mechanisms with vector-difference-driven refinement in the same optimization cycle.

1.4 Paper Organization

The remainder of this paper is organized as follows. Section 2 outlines the main principles of the proposed HSFOADE algorithm. Section 3 presents the theoretical background of IIR system identification and experimental setup and discusses the benchmark IIR systems considered, followed by comparative evaluations of HSFOADE against baseline algorithms and methods reported in the literature. Section 4 discusses the obtained results, with emphasis on convergence behaviour, coefficient accuracy, computational cost, and the limitations of the study. Section 5 concludes the paper by summarizing the main findings and contributions and by outlining directions for future research.

2 Proposed Hybrid Starfish Optimization Algorithm with Differential Evolution

2.1 Starfish Optimization Algorithm

SFOA [37] is a bio-inspired metaheuristic that mimics three main behaviours of starfish: exploration, preying, and regeneration, as shown in Fig. 1. The algorithm begins with a random initialization of the population $X \in \mathbb{R}^{N\times D}$, where each starfish position is defined as:

$$X_{ij} = l_j + r \cdot \left(u_j - l_j\right), i = 1, \ldots, N; j = 1, \ldots, D \tag{1}$$

with $r \sim U(0,1)$ and u_j, l_j as the bounds, after initialization, In SFOA, exploration and exploitation phases are selected probabilistically with equal likelihood at each iteration. For higher-dimensional problems ($D > 5$), a five-dimensional arm search is performed by updating five randomly chosen dimensions:

$$Y_{i,p}^T = X_{i,p}^T + a_1 \left(X_{best,p}^T - X_{i,p}^T\right) \times \cos(\theta), r \le 0.5 \tag{2}$$

$$Y_{i,p}^T = X_{i,p}^T - a_1 \left(X_{best,p}^T - X_{i,p}^T\right) \times \sin(\theta), r > 0.5 \tag{3}$$

where $a_1 = (2r-1)\pi$, and $\theta = \frac{\pi}{2}\frac{T}{T_{max}}$. For lower-dimensional problems ($D \le 5$), a unidimensional update is applied:

$$Y_{i,q}^T = E^t X_{i,p}^T + A_1 \left(X_{k1,p}^T - X_{i,p}^T\right) + A_2 \left(X_{k2,p}^T - X_{i,p}^T\right) \tag{4}$$

where $A_1, A_2 \sim U(-1,1)$, and the energy factor is given as follows.

$$E^t = \frac{T_{max} - T}{T_{max}} \times \cos(\theta) \tag{5}$$

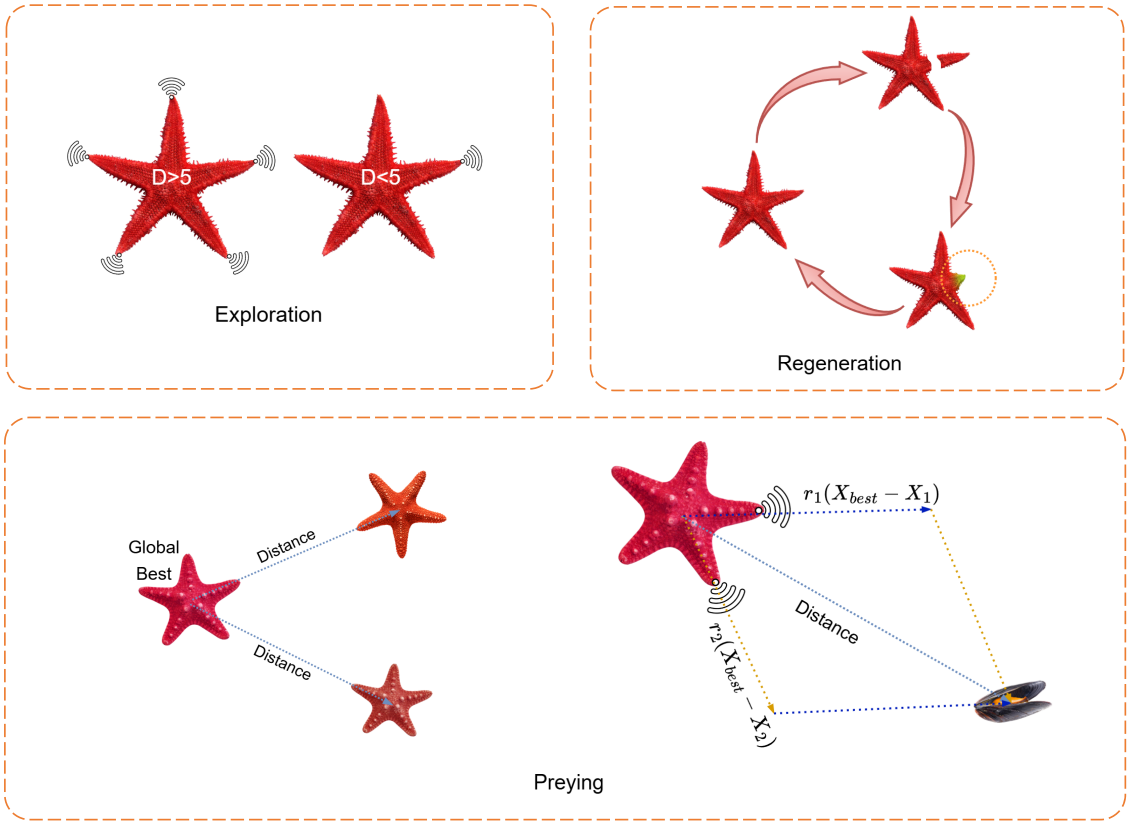

Figure 1: Exploration, preying, and regeneration behaviours of starfish as inspiration for SFOA.

This mechanism regulates the interaction between exploration efficiency and local diversification. The exploitation phase is modelled by preying and regeneration. In preying, each starfish computes distances to the global best (given in Eq. (6)):

$$d_m = X_{best}^T - X_{m,p}^T, \quad m = 1, \ldots, 5 \tag{6}$$

and randomly selects two distances to update its position with a parallel two-directional strategy given as follows.

$$Y_i^T = X_i^T + r_1 d_{m1} + r_2 d_{m2}, \quad r_1, r_2 \sim U(0,1) \tag{7}$$

This ensures both attraction toward promising regions and repulsion to maintain diversity. Regeneration is applied only to the last starfish in the population ($i = N$), modelling the biological arm regrowth:

$$Y_i^T = \exp\left(-\frac{T \cdot N}{T_{max}}\right) X_i^T, \tag{8}$$

a step that strengthens global convergence by avoiding stagnation in local minima. For all updates, boundary conditions are enforced as given in Eq. (9).

$$X_i^{T+1} = \begin{cases} lb & Y_i^T < lb \\ ub & Y_i^T > ub \\ Y_i^T & otherwise \end{cases} \tag{9}$$

The main loop continues until the maximum iteration T_{max} reached, and the best fitness is recorded. Through its hybrid dimensional search, parallel two-directional preying, and regeneration mechanism, SFOA achieves a balanced exploration–exploitation trade-off and demonstrates competitive global optimization performance across diverse benchmarks.

2.2 Differential Evolution

DE is a population-based stochastic optimization algorithm introduced by Storn and Price in 1997 [77], designed for solving continuous nonlinear and non-differentiable optimization problems. Like other evolutionary algorithms, DE maintains a population of candidate solutions $X = \{x_1, x_2, \ldots, x_N\}$, where each $x_i \in \mathbb{R}^D$ represents a potential solution in a D-dimensional search space.

Unlike classical genetic algorithms that rely on predefined crossover and mutation operators, DE employs a unique differential mutation and recombination strategy that exploits differences between individuals to generate new candidate solutions. For each target vector x_i^t in generation t, a mutant vector is created by perturbing the population through scaled differences of randomly selected individuals:

$$v_i^t = x_{r1}^t + F \cdot (x_{r2}^t - x_{r3}^t) \tag{10}$$

where $r_1, r_2, r_3 \in \{1, 2, \ldots, N\}$ are distinct indices different from i, and $F \in (0, 2)$ is a scaling factor controlling the amplification of differential variations. This mechanism ensures self-adaptive step sizes and maintains diversity across the search space. To increase the strength of the method, DE applies a binomial crossover to mix the target vector and its mutant:

$$u_i^{t+1} = \begin{cases} v_i^t, & if\ rand_j \le CRorj = j_{rand}, \\ x_i^t, & otherwise, \end{cases} \tag{11}$$

where $CR \in [0, 1]$ is the crossover rate, $rand_j \sim U(0, 1)$ is a uniform random number, and j_{rand} ensures at least one element is inherited from the mutant. The resulting trial vector u_i^t is then evaluated against the target vector using greedy selection:

$$x_i^{t+1} = \begin{cases} u_i^t, & f(u_i^t) \le f(x_i^t), \\ x_i^t, & otherwise, \end{cases} \tag{12}$$

where (x_i^t) denotes the objective function. This selection mechanism guarantees that the population does not deteriorate and continuously evolves toward better solutions. The iterative cycle of mutation, crossover, and selection continues until a stopping criterion, typically the maximum number of generations or a convergence threshold, is met. DE's main advantages are its conceptual simplicity, few control parameters (population size N, scaling factor F, and crossover rate CR), and its strong performance on high-dimensional and multimodal functions. It has become a widely used algorithm in global optimization and engineering applications due to its balance of exploration and exploitation and its ability to escape local minima without requiring gradient information [77–79].

2.3 Hybridization of SFOA and DE

Hybridization strategies in metaheuristic optimization are designed to integrate distinct operators within a unified framework in order to enhance search performance. SFOA relies on probabilistic selection between exploration and exploitation phases, incorporating a hybrid dimensional search and regeneration to preserve diversity, while DE employs differential mutation, crossover, and greedy selection to ensure

substantial variation and elitist replacement. The proposed HSFOADE combines these mechanisms under a single iterative process, allowing SFOA's stochastic exploration–exploitation balance to be reinforced by the adaptive variation and selection scheme of DE.

In the proposed HSFOADE, the hybridization is not implemented as a mutually exclusive switching mechanism between SFOA and DE. Instead, DE is embedded as a refinement layer within each iteration. Specifically, each iteration begins with DE-based mutation, crossover, and greedy selection applied to the entire population. The updated population is then processed by the SFOA component, where the control parameter G_p governs only the probabilistic selection between exploration and exploitation phases. Therefore, the proposed method follows a sequential embedded hybrid structure, in which DE provides difference-based directional refinement, while SFOA maintains population diversity and global search capability.

The parameter G_p controls the probabilistic selection between the exploration and exploitation phases within the SFOA component. In this study, G_p is set to 0.5 to maintain statistical neutrality between these two phases. This choice avoids introducing a bias toward either exploration or exploitation, which is particularly important in problems where the landscape characteristics are not known a priori. By assigning equal probability, the algorithm allows both mechanisms to operate with comparable frequency, enabling a balanced search process. It is important to note that G_p does not control the activation of the DE component, which is embedded in every iteration as a refinement mechanism.

In the SFOA component, exploration or exploitation is selected with equal probability. When exploration phase is selected, the search is dimension-dependent: if the problem dimension is greater than five, a five-dimensional update based on trigonometric arm movements is performed, while for dimensions of five or less, a unidimensional update guided by peer differences and an energy-scheduling factor is applied. When exploitation is selected, all starfish perform the preying update using two randomly chosen distances to the global best. At the same time, the last individual in the population undergoes regeneration with an exponential update rule. Boundary conditions are checked after each move to ensure feasibility.

In the embedded DE refinement layer, a mutant vector is generated through differential mutation, and a trial vector is constructed using binomial crossover with crossover rate CR. The trial vector is then evaluated and compared with its target vector using greedy selection, ensuring that the population never deteriorates. This step provides substantial variation and guarantees elitism in the search process.

The incorporation of DE operators is not intended as a simple augmentation, but as a structural modification of the update mechanism. While SFOA provides stochastic exploration and population diversity, it lacks a systematic mechanism for directional refinement. The DE component compensates for this limitation by introducing difference-based mutation and greedy selection, which guide the search toward promising regions with controlled step sizes. This combination alters the search dynamics by reducing randomness in later stages while maintaining sufficient diversity in early iterations. The essential distinction of HSFOADE is that DE is not used as an independent optimizer or a post-processing step. It is embedded into the iterative population evolution of SFOA as a directional refinement layer. Therefore, each population update first receives difference-based guidance through mutation, crossover, and greedy selection, and then evolves through the exploration, preying, or regeneration mechanisms of SFOA. This sequential interaction changes the search trajectory of the original SFOA and provides a mechanism-level contribution rather than a direct operator aggregation.

While the operational details of DE are described in Section 2.2, its role within the proposed framework is to compensate for a specific limitation of SFOA. The update mechanism of SFOA is primarily driven by stochastic perturbations and attraction strategies, which do not explicitly utilize relative differences between

candidate solutions. This restricts its ability to perform consistent directional refinement in later iterations. Within HSFOADE, DE operators are not introduced as standalone components, but as a targeted mechanism to incorporate difference-based guidance into the update process. This enables the algorithm to exploit population structure more effectively, leading to more stable refinement of candidate solutions, particularly in regions where precise coefficient adjustment is required.

After the embedded DE refinement and the SFOA update are completed, the population is evaluated, and the best solution of the current iteration is recorded. By applying DE refinement before the SFOA exploration–exploitation update in each iteration, HSFOADE combines difference-based directional refinement with population-diversity preservation. This integration enforces a coordinated interaction between global exploration and local exploitation, making HSFOADE a competitive choice for complex optimization problems.

The proposed hybrid method, HSFOADE, is constructed by embedding DE operators into the main loop of the SFOA. As illustrated in the pseudocode block above (Algorithm 1) and shown in the flowchart in Fig. 2, the algorithm begins with the standard SFOA framework, where exploration and exploitation phases are executed based on the parameter Gp. At the beginning of each iteration, DE mutation and crossover are applied to generate trial vectors, which are then evaluated using greedy selection followed by boundary checks. This integration allows the algorithm to maintain SFOA's biologically inspired search dynamics while benefiting from DE's efficient variation operators, producing a more balanced optimization process [37,78]. In this study, standard DE control parameters (scaling factor F and crossover rate CR) are adopted without additional adaptation in order to isolate the effect of the hybrid structure and ensure fair comparison across methods.

Algorithm 1: Pseudocode for HSFOADE

```
Input: Algorithmic parameters (N, Tmax, and Gp)
Output: The global solution
01: Initialize input parameters, problem information, boundary, etc.
02: Initialize positions and evaluate the fitness values
03: While T < Tmax Do
04:       For each starfish Do       %% DE start
05:            Select three distinct indices r1, r2, r3 ≠ i
06:            Generate mutant vector v = X[r1] + F*(X[r2] − X[r3])
07:            Perform binomial crossover with rate CR to form trial u
08:            Evaluate fitness f(u)
09:            If f(u) ≤ f(X[i]) then X[i] = u      % greedy selection
10:            Apply boundary check on X[i]
11:       End For                                   %% DE end
12:       If rand > Gp % Exploration phase
13:            Calculate θ and energy Et
14:            For each starfish Do
15:                 If D > 5 Do % When the dimension is larger than 5
16:                      Generate five randomly p-dimensions among D
17:                      For j = 1:5 Do % Update five randomly selected p-dimensions
18:                           Calculate a1
19:                           Update the dimension of position in starfish
20:                      End For
```

(Continued)

Algorithm 1 (continued)

```
                Else % When the dimension is not larger than 5
                    Generate two random numbers A1 and A2
                    Select a random dimension p
                    Update the p-dimension of position using
                    Check the boundary of starfish
                End If
            End For
        Else % Exploitation phase
            Generate distances between the best position and starfish
            For each starfish Do
                Generate random number rk, and update the position using
                If i = N Do
                    Update the position % regeneration phase
                End If
                Check the boundary of starfish by
            End For
        End If % Updating finished
        Calculate the fitness values for all starfish % Obtain fitness values
        Obtain the global best solution in iteration T step
        T = T + 1
End While
Obtain global solution
```

2.4 Discussion of the Algorithmic Behaviour

To provide an explanation beyond numerical observations, the behaviour of the proposed method is analysed in terms of its update dynamics. The search process of HSFOADE is governed by the interaction between stochastic exploration and difference-based refinement (DE). In SFOA, candidate solutions are updated using stochastic trigonometric perturbations and distance-based attraction toward reference points. This mechanism maintains population diversity and enables wide coverage of the search space; however, the update directions are largely random and do not explicitly exploit relative information between individuals. As a result, refinement in later iterations may remain inefficient, particularly in multimodal error landscapes.

The DE component introduces a structured update of the form $x_i^{t+1} = x_r^t + F(x_p^t - x_q^t)$, where the difference between individuals provides directional information. This operation implicitly adapts the step size according to population dispersion: larger differences in early iterations promote exploration, while smaller differences in later stages lead to localized refinement. The subsequent greedy selection mechanism ensures that only improving solutions are retained, leading to a gradual reduction of population variance. The combined effect of these mechanisms results in a two-phase search behaviour. In early iterations, diversity is preserved through stochastic updates, preventing premature convergence. In later iterations, the influence of difference-based updates becomes dominant, enabling controlled and stable refinement. This behaviour is particularly relevant for IIR system identification, where accurate estimation of denominator coefficients requires both global exploration and precise local adjustment.

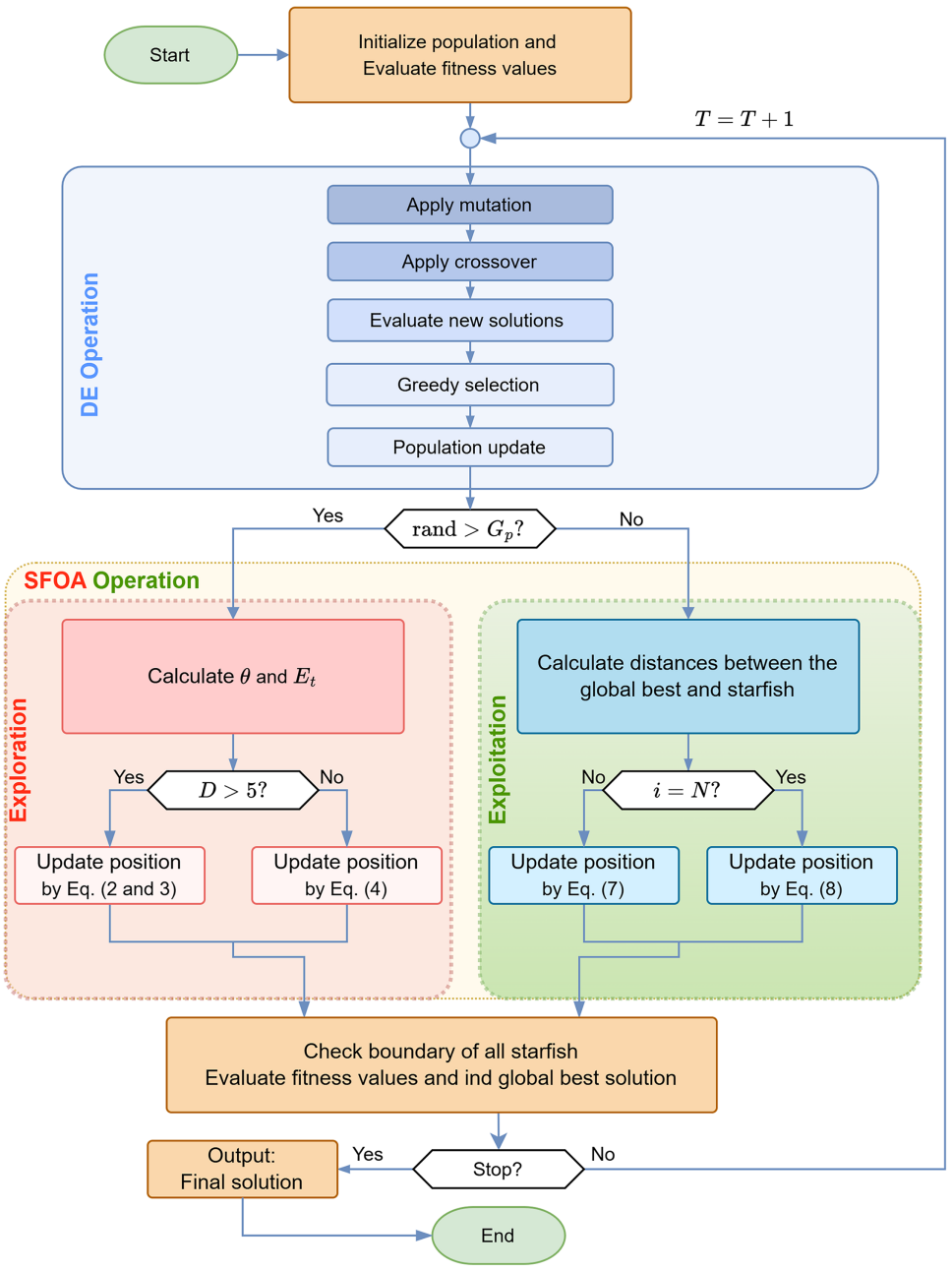

Figure 2: Flowchart of HSFOADE.

The scalability of HSFOADE is primarily governed by its population-based structure and the linear dependence of update operations on the number of decision variables. The difference-based mutation in DE operates directly in the solution space without requiring gradient information, allowing the method to maintain its functionality as the problem dimension increases. In addition, the stochastic exploration mechanism of SFOA preserves diversity across larger search spaces, reducing the risk of premature convergence. In terms of generalizability, the algorithm does not rely on problem-specific assumptions and operates solely on objective function evaluations. Therefore, it can be applied to a broad class of continuous optimization problems beyond IIR system identification, provided that the objective function is well-defined.

2.5 Computational Complexity Analysis

The computational cost of the proposed method can be analysed from two perspectives: objective-function evaluations and arithmetic update operations.

From the evaluation perspective, both SFOA and HSFOADE perform one objective-function evaluation for each individual at each iteration. Therefore, for a population size of N and a maximum iteration number of T, the total number of objective-function evaluations is $(N \times T)$. This gives an evaluation complexity of $\mathcal{O}(NT)$ for both algorithms.

From the arithmetic perspective, the position updates of SFOA require vector-based operations over the decision dimension D. In HSFOADE, the embedded DE mutation, crossover, and greedy selection operations also operate on D-dimensional candidate vectors. Therefore, the arithmetic update cost remains proportional to $N \times T \times D$, leading to an overall update complexity of $\mathcal{O}(NTD)$.

The additional DE layer increases the number of vector operations inside each iteration but does not increase the number of objective-function evaluations. Since IIR system identification requires signal simulation and mean-squared-error computation during each objective evaluation, the evaluation cost is the dominant component of the total computational burden. Therefore, HSFOADE introduces only a limited arithmetic overhead while preserving the same asymptotic evaluation complexity as SFOA.

3 Comparative Study of HSFOADE and Baseline Optimizers in IIR Filter Design

This section presents a comparative evaluation of the proposed HSFOADE algorithm against baseline optimizers in the context of IIR filter design. A direct comparison with the baseline SFOA results highlights the contribution of the hybrid structure, particularly the role of DE-based refinement in improving update quality. All algorithms are initialized using uniform random sampling within the predefined bounds, and identical parameter settings are used to ensure a fair comparison. Performance is evaluated in terms of convergence behaviour and final mean squared error (MSE) values.

3.1 IIR System Definition

FIR and IIR filters are the two fundamental categories of digital filters, each with distinct mathematical formulations and structural characteristics. FIR filters are defined by a finite-duration impulse response and are implemented through non-recursive structures, which makes them inherently stable and capable of achieving exact linear-phase behaviour. However, these advantages often come at the expense of high filter order and increased computational cost. By contrast, IIR filters employ recursive feedback, resulting in an impulse response that extends indefinitely and allowing them to approximate desired frequency responses with much lower order and reduced computational load. This efficiency makes IIR filters attractive in real-time applications, though they must be carefully designed to avoid instability and phase distortion. Both classes are traditionally represented by transfer functions and block diagrams that illustrate their difference equations and system structures, serving as the mathematical and schematic basis for further developments. Building upon these foundations, the subsequent sections focus on application-oriented designs where IIR filters are optimized using advanced metaheuristic algorithms to enhance performance, ensure stability, and meet practical constraints in complex engineering environments.

In the adaptive IIR filter identification problem, the goal is to approximate the behaviour of an unknown system using a parametric IIR model whose coefficients are tuned iteratively. The output of the unknown IIR filter can be expressed as:

$$d(k) = \frac{\sum_{i=0}^{M} m_i x(k-i)}{1 + \sum_{j=1}^{N} n_j y(k-j)} \tag{13}$$

where $x(k)$ is the input, $d(k)$ is the desired (unknown system) output, m_i are the numerator coefficients, and n_j are the denominator coefficients of the target IIR system. The adaptive IIR filter, driven by the same input signal $x(k)$, produces an estimated output:

$$\hat{d}(k) = \frac{\sum_{i=0}^{M} \hat{m}_i x(k-i)}{1 + \sum_{j=1}^{N} \hat{n}_j \hat{y}(k-j)} \tag{14}$$

with estimated coefficients $\hat{m}_i$ and $\hat{n}_j$. The modelling error at time k is then obtained as follows.

$$e(k) = d(k) - y(k) \tag{15}$$

The objective of the identification problem is to minimize the mean squared error (MSE):

$$J(\theta) = \frac{1}{K} \sum_{k=1}^{K} e^2(k) \tag{16}$$

where $\theta = [\hat{m}_0, \hat{m}_1, \ldots, \hat{m}_n, \hat{n}_1, \ldots, \hat{n}_n]^T$ is the coefficient vector. Because the cost surface of IIR filter identification is nonlinear and multimodal, gradient-based methods often converge to local minima. To address this, the optimization block in Fig. 3 employs bio-inspired metaheuristic algorithms such as the SFOA and the HSFOADE. These algorithms update the coefficient vector θ iteratively:

$$\theta^{(t+1)} = \theta^{(t)} + \Delta\theta^{(t)}, \tag{17}$$

where $\Delta\theta^{(t)}$ is generated according to the exploration–exploitation strategies of the chosen optimizer. This iterative adaptation ensures that the estimated filter gradually converges toward the behavior of the unknown IIR system while maintaining stability and improving accuracy.

3.2 Experimental Setup

To evaluate the effectiveness of the proposed HSFOADE algorithm in IIR filter identification, a set of controlled experiments was conducted under standardized conditions. The input signal $x(k)$ (Fig. 4) used throughout the study is a uniformly distributed white noise sequence with an amplitude range of $[-0.5, 0.5]$, ensuring persistent excitation of the unknown system across all frequency components. Each optimization run was executed for a maximum of 1000 iterations with a fixed population size of 40 individuals. To ensure statistical reliability and strength of the reported results, all algorithms were independently executed over 25 trials, and their performance was assessed in terms of best, worst, mean, and standard deviation of the MSE. All algorithms are executed under identical initialization and evaluation settings. The same input–output data pair, coefficient bounds, and stopping criteria are applied across all runs, and no additional parameter tuning is introduced for individual methods. At each iteration, candidate solutions are evaluated using the same error formulation and sampling structure. Boundary handling is enforced immediately after each update to prevent infeasible coefficient values. This setup isolates the effect of the search mechanism, allowing performance differences to be attributed directly to the update dynamics of the algorithms. In this study, the DE control parameters were fixed at ($F = 0.5$) and ($CR = 0.7$). These values are among the most commonly used parameter settings in the DE literature and have been widely reported to provide a good balance between exploration and exploitation. Therefore, they were adopted in the proposed algorithm to ensure stable performance and fair evaluation across all benchmark functions. In all IIR filter examples, the numerator and denominator coefficients were considered within the range of −2 to 2.

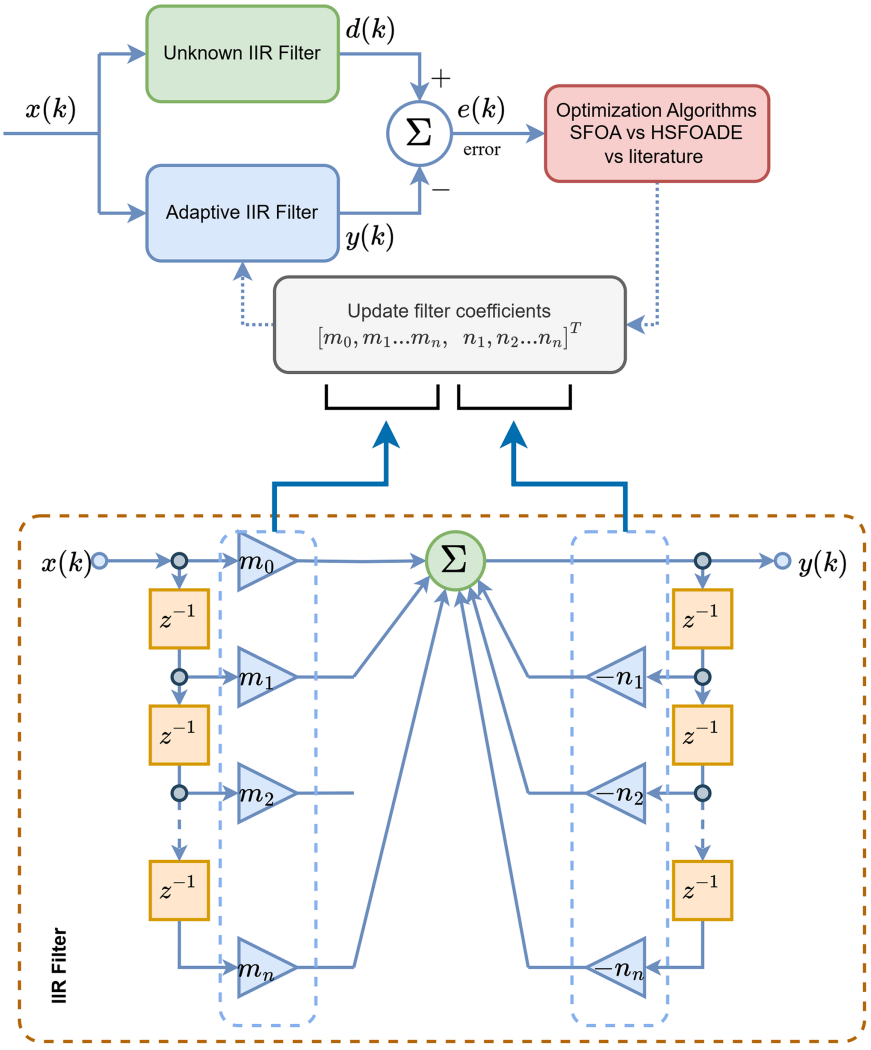

Figure 3: Complete schematic representation for optimized IIR filter test system.

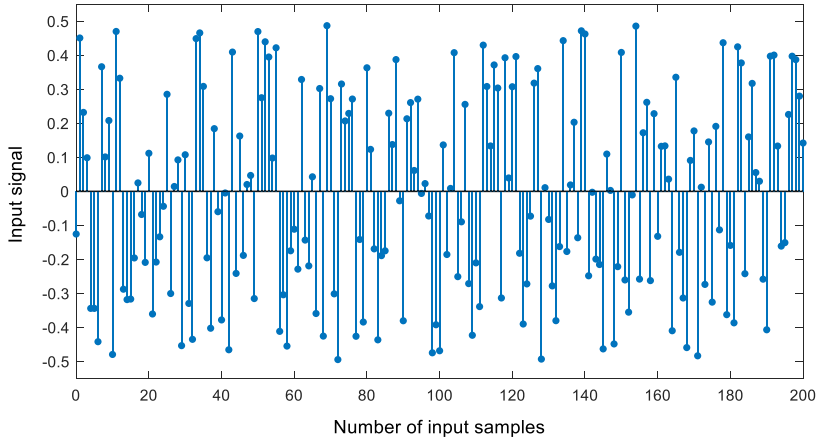

Figure 4: The input signal $x(k)$ is a uniformly distributed white noise sequence with an amplitude of $[-0.5, 0.5]$.

The comparative analysis involved the proposed HSFOADE alongside the original SFOA [37] and three well-established baseline optimizers from the recent literature: the animated oat optimization (AOO) [80], the mountain gazelle optimizer (MGO) [81], and the slime mould algorithm (SMA) [82]. These algorithms were selected because their effectiveness has been consistently demonstrated in the optimization literature, where they are frequently employed as strong benchmark methods in comparative studies. By adopting well-validated reference algorithms directly from the literature, the evaluation remains aligned with established benchmarking practices. This selection enables both a direct assessment of the improvement achieved over the original SFOA and a comparison against representative metaheuristics from different algorithmic families. The overall workflow of the identification process, including signal generation, adaptive filtering, and optimization-driven coefficient updates, is illustrated in Fig. 3. In addition to these directly implemented baselines, stronger DE-based and hybrid metaheuristic methods reported in the literature, including DE, ADE, ADE-LS, GOASA, QPSO, and HPSO-GSA, are also considered in Section 3.4.3 to provide a broader comparison against advanced optimization frameworks.

3.3 Example System 1: Second-Order IIR (Same- and Reduced-Order)

The first identification example considers a second-order IIR system to evaluate the basic convergence and coefficient estimation capability of the proposed HSFOADE algorithm. This system provides a compact but informative test case because it contains recursive denominator dynamics and a nontrivial pole–zero structure. Both same-order and reduced-order identification scenarios are examined under identical input, population size, iteration number, and statistical protocol. The same-order case evaluates whether the algorithms can recover the original system parameters when the model structure matches the target system. The reduced-order case introduces a structural mismatch and therefore assesses the ability of each optimizer to approximate the dominant system behaviour with fewer parameters. Through these two settings, the second-order example provides a controlled basis for comparing convergence behaviour, estimation accuracy, and error consistency among HSFOADE and the baseline optimizers.

Eq. (18) defines the transfer function of the second-order IIR system employed as the benchmark model in this study. The system includes both numerator and denominator dynamics, ensuring the presence of recursive feedback and a nontrivial pole–zero structure that makes the identification problem challenging. The denominator coefficients define two distinct real poles located at approximately $(z = 0.8303)$ and $(z = 0.3011)$. Since both pole magnitudes are smaller than unity, the discrete-time system satisfies the stability condition in the (z)-domain. By attempting to recover these coefficients through optimization, the experiment directly evaluates the capacity of HSFOADE and the comparative algorithms to navigate a multimodal error surface, achieve accurate pole–zero estimation, and minimize the mean squared error between the actual and estimated outputs.

$$H_1\left(z^{-1}\right) = \frac{0.05 - 0.4z^{-1}}{1 - 1.1314z^{-1} + 0.25z^{-2}} \tag{18}$$

3.3.1 Same-Order System

Eq. (19) defines the same-order parametric model employed to identify the second-order IIR system, ensuring that the assumed filter structure exactly matches the actual system dynamics. The performance comparison is illustrated in Fig. 5, where the MSE values (in dB) are summarized for all algorithms. The proposed HSFOADE clearly achieves the lowest error, with its distribution tightly clustered near −320 dB, indicating both accuracy and stability in coefficient estimation. In contrast, the original SFOA attains median values around −200 dB, while AOO and MGO converge more slowly with error levels near −100 and −80 dB, respectively. SMA exhibits the weakest performance, stabilizing close to −60 dB with higher variance.

These results confirm that embedding DE operators within the starfish framework significantly enhances identification quality, producing near-zero error in same-order modelling scenarios.

$$H_{1,same}\left(z^{-1}\right) = \frac{b_0 + b_1 z^{-1}}{1 - a_1 z^{-1} - a_2 z^{-2}} \tag{19}$$

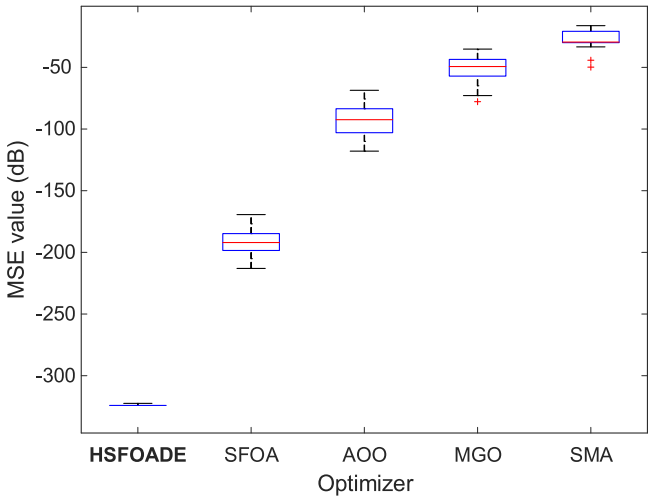

Figure 5: MSE distribution for same-order IIR system identification using HSFOADE and baseline optimizers.

The statistical outcomes for the same-order identification of the second-order IIR system are reported in Table 2, while the convergence profiles are illustrated in Fig. 6. As observed, HSFOADE achieves the best performance with a mean squared error approaching zero ($best = 0$, $mean \approx 1.61 \times 10^{-33}$) and an extremely low standard deviation (2.15×10^{-33}), indicating both accuracy and stability. In comparison, SFOA reaches a mean error on the order of 10^{-18}, whereas AOO, MGO, and SMA converge to substantially higher values (10^{-8}, 10^{-5}, and 10^{-3}, respectively), reflecting weaker identification capability. The superiority of HSFOADE is further confirmed by the p-values (from nonparametric Wilcoxon test), which demonstrate statistically significant improvements over all baseline methods.

Table 2: Statistical performance of same-order IIR system identification across 25 runs, including nonparametric Wilcoxon signed-rank test results (p-values).

Statistical Measure	HSFOADE	SFOA	AOO	MGO	SMA
Best	**0**	4.9855E−22	1.6150E−12	1.6520E−08	1.0462E−05
Worst	**5.7414E−33**	1.1570E−17	1.3814E−07	3.0313E−04	2.4169E−02
Mean	**1.6164E−33**	1.1764E−18	1.1268E−08	3.2715E−05	6.0961E−03
SD	**2.1500E−33**	3.0757E−18	2.9325E−08	6.1610E−05	8.9370E−03
p-value	—	1.2290E−05	1.2290E−05	1.2290E−05	1.2290E−05

The bold values indicate the best (lowest) results obtained among the compared algorithms for each statistical measure (Best, Worst, Mean, and SD).

Fig. 6 provides a complementary view of the optimization dynamics, where HSFOADE exhibits the fastest and most stable decline in error, steadily approaching the global optimum. At the same time, other algorithms stagnate at considerably higher error floors. Together, these results validate the effectiveness of the hybrid approach in delivering both rapid convergence and accuracy in same-order IIR system modelling.

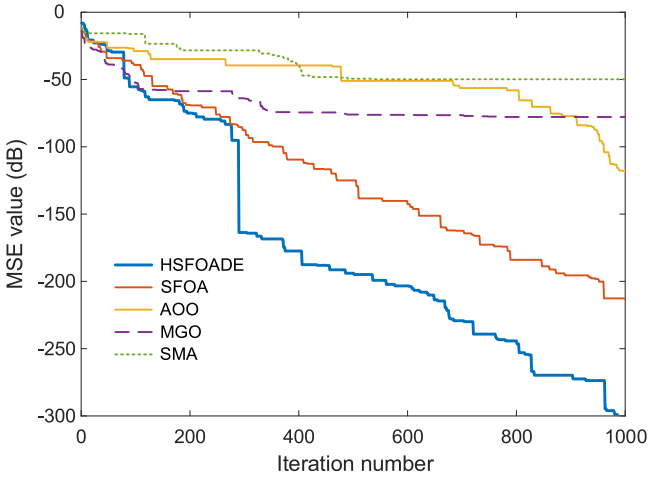

Figure 6: Convergence curves of MSE values for the same-order IIR system identification.

The coefficient estimates reported in Table 3 confirm that HSFOADE exactly reproduces the actual parameter values of the second-order IIR system, achieving perfect identification in the same-order scenario. In contrast, while SFOA and AOO provide close approximations, MGO and SMA introduce minor deviations, particularly in the denominator terms. Table 4 further highlights this distinction by presenting the absolute errors: HSFOADE yields zero error across all coefficients, whereas the competing algorithms exhibit varying levels of mismatch, with SMA producing the most significant deviations.

Table 3: Estimated coefficients of the same-order IIR system compared with real values.

Coefficient	Real Value	Estimated Value				
		HSFOADE	SFOA	AOO	MGO	SMA
a_1	1.1314	1.1314	1.1314	1.1314	1.1325	1.1071
a_2	−0.25	−0.2500	−0.2500	−0.2500	−0.2510	−0.2285
b_0	0.05	0.0500	0.0500	0.0500	0.0499	0.0563
b_1	−0.4	−0.4000	−0.4000	−0.400	−0.3995	−0.4144

Table 4: Absolute estimation errors for the coefficients of the same-order IIR system.

Coefficient	Absolute Error = |Real Value − Estimated Value|				
	HSFOADE	SFOA	AOO	MGO	SMA
a_1	0	1.0460E−10	9.0703E−06	1.0651E−03	2.4274E−02
a_2	0	1.0759E−10	8.0101E−06	9.6276E−04	2.1521E−02
b_0	0	4.0518E−11	1.6773E−06	1.4337E−04	6.3352E−03
b_1	0	5.5971E−11	5.5491E−06	5.0820E−04	1.4392E−02

3.3.2 Reduced-Order System

Eq. (20) defines the reduced-order IIR model, where the system structure is intentionally chosen with fewer parameters than the accurate second-order reference. This mismatch introduces approximation

error, making the identification task more challenging and providing a means to assess the impact of different optimizers under model-order reduction. The comparative results summarized in Fig. 7 reveal that HSFOADE consistently achieves the lowest mean squared error among all tested algorithms, with its distribution concentrated near 1.1×10^{-2} (≈−19.3 dB). In contrast, SFOA, AOO, and MGO converge to higher error levels, while SMA exhibits the weakest performance with broader variance. These findings demonstrate that, even under reduced-order conditions, HSFOADE maintains superior convergence behaviour and delivers more accurate approximations of the system dynamics compared to competing methods.

$$H_{1,reduced}\left(z^{-1}\right) = \frac{b_0}{1 - a_1 z^{-1}} \tag{20}$$

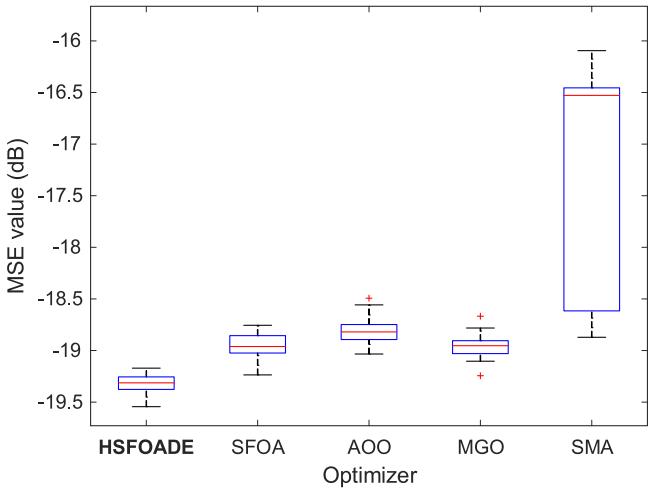

Figure 7: MSE distribution for reduced-order IIR system identification using HSFOADE and baseline optimizers.

Table 5 and Fig. 8 present the results of the reduced-order identification scenario. HSFOADE delivers the best statistical outcomes with a mean MSE of 1.1692×10^{-2} and a standard deviation of 2.46×10^{-4}, clearly outperforming all baselines. SFOA, AOO, and MGO yield higher mean errors in the range of 1.27×10^{-2} to 1.31×10^{-2} with larger deviations, while SMA performs the weakest with a mean of 1.94×10^{-2} and the most significant variance. The convergence curves in Fig. 8 confirm this behaviour, showing HSFOADE's rapid descent and stable plateau compared to the slower and noisier trajectories of the competing algorithms.

Table 5: Statistical performance of reduced-order IIR system identification across 25 runs, including nonparametric Wilcoxon signed-rank test results (p-values).

Statistical Measure	HSFOADE	SFOA	AOO	MGO	SMA
Best	1.1107E−02	1.1923E−02	1.2492E−02	1.1901E−02	1.2967E−02
Worst	1.2104E−02	1.3318E−02	1.4148E−02	1.3591E−02	2.4577E−02
Mean	1.1692E−02	1.2766E−02	1.3156E−02	1.2724E−02	1.9395E−02
SD	2.4661E−04	3.3866E−04	4.1340E−04	3.5108E−04	4.4613E−03
p-value	—	1.2290E−05	1.2279E−05	1.2290E−05	1.2290E−05

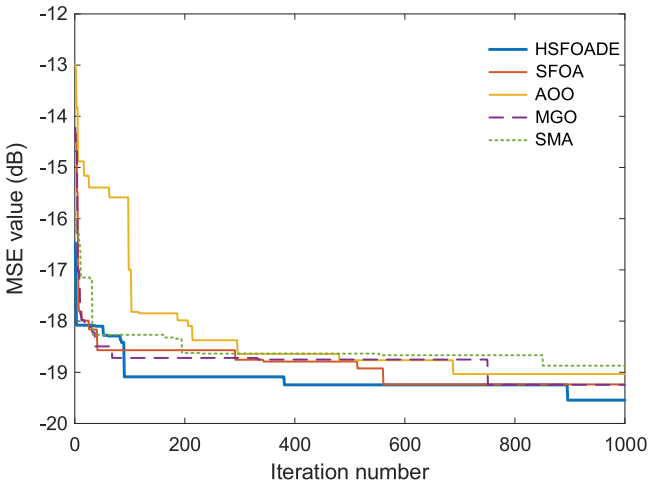

Figure 8: Convergence curves of MSE values for reduced-order IIR system identification.

Table 6 lists the estimated coefficients for the reduced-order IIR system. HSFOADE provides values closest to the actual parameters, with only minimal deviations, while SFOA achieves slightly less accurate estimates. AOO and MGO show noticeable drifts in both numerator and denominator terms, and SMA produces the most considerable discrepancies. These results highlight HSFOADE's superior ability to preserve the dominant dynamics under order reduction.

Table 6: Estimated coefficients of the reduced-order IIR system obtained by different optimizers.

Coefficient	Estimated Value				
	HSFOADE	**SFOA**	**AOO**	**MGO**	**SMA**
a_1	0.9244	0.9234	0.9167	0.9081	0.9047
b_0	−0.2625	−0.2850	−0.2819	−0.2462	−0.3084

3.3.3 Comparison with Reported Works

To further validate the effectiveness of the proposed HSFOADE, its performance is compared with several optimization methods previously reported in the literature. For the same-order IIR system identification, Table 7 shows that HSFOADE achieves the lowest error levels, with best and mean MSE values approaching zero and a tiny standard deviation (2.15×10^{-33}). In comparison, atom search optimization (ASO), moth flame optimization (MFO), GSA [63], opposition-based hybrid coral reefs optimization (OHCRO) [66] and improved cooperative particle swarm optimization with multi-swarm (ICPSO-MS) [66] produce higher error values and larger variances. While some of these algorithms demonstrate competitive accuracy in specific runs (e.g., OHCRO best case 1.93×10^{-15}) Their average performance remains weaker than HSFOADE. These results indicate that the hybrid integration of starfish dynamics with DE provides a more consistent and reliable framework for same-order IIR filter modelling.

For the reduced-order system, HSFOADE also shows superior results compared to other optimizers in Table 7. It means MSE of 1.17×10^{-2} is lower than ASO (1.21×10^{-2}) and MFO (1.22×10^{-2}), while classical approaches like GSA (1.46×10^{-2}), OHCRO (1.60×10^{-1}), and ICPSO-MS (1.60×10^{-1}) fall behind by a significant margin. The lower standard deviation of HSFOADE confirms that its performance is not only

accurate but also stable across independent trials. This demonstrates that the proposed algorithm maintains its advantage even under reduced-order modelling, where approximation error is unavoidable, proving its strength and adaptability compared with well-established methods in the literature.

Table 7: Comparative performance of HSFOADE and reported optimizers for exact- and reduced-order IIR system identification.

Type	Reference	Optimizer	MSE			
			Best	Worst	Mean	SD
Same-order	This study	HSFOADE	0	5.7414E−33	1.6164E−33	2.1500E−33
	[63]	ASO	6.1032E−26	3.4896E−23	8.5799E−24	8.9133E−24
	[63]	MFO	4.6466E−15	6.0558E−08	7.7854E−09	1.5518E−08
	[63]	GSA	3.1619E−05	2.0703E−03	5.2445E−04	4.8648E−04
	[66]	OHCRO	1.93E−15	1.48E−09	7.53E−11	2.62E−10
	[66]	ICPSO-MS	8.83E−14	7.79E−05	1.96E−06	1.90E−06
Reduced-order	This study	HSFOADE	1.1107E−02	1.2104E−02	1.1692E−02	2.4661E−04
	[63]	ASO	1.1436E−02	1.2390E−02	1.2115E−02	2.3867E−04
	[63]	MFO	1.1566E−02	1.2714E−02	1.2249E−02	2.7452E−04
	[63]	GSA	1.2054E−02	1.8893E−02	1.4632E−02	2.2303E−03
	[66]	OHCRO	0.1320	0.1954	0.1605	0.0134
	[66]	ICPSO-MS	0.1359	0.1848	0.1607	0.0139

3.4 Example System 2: Fifth-Order IIR (Same- and Reduced-Order)

We next examine a more challenging fifth-order IIR system shown in (21) to evaluate scalability and stability under higher dimensionality. With identical input, run budget, and statistical protocol, HSFOADE again demonstrates superior convergence behaviour, reaching markedly lower MSE levels and exhibiting narrower run-to-run variability than all baselines. The same-order identification highlights HSFOADE's advantage in navigating the multimodal error surface: denominator coefficients are estimated with minimal absolute deviations, yielding stable realizations and accurate magnitude/phase responses. Under reduced-order modelling, error floors naturally rise; yet HSFOADE sustains the best compromise between fit quality and parameter economy, preserving the main poles while attenuating spurious dynamics. Across both systems and modelling regimes, qualitative inspection of convergence curves and quantitative summaries; best, worst, mean and SD (standard deviation) consistently favour the proposed hybrid, underscoring the value of combining SFOA's exploration–exploitation balance with DE-style variation and elitist replacement within a single iterative loop.

$$H_2\left(z^{-1}\right) = \frac{0.1084 + 0.5419z^{-1} + 1.0837z^{-2} + 1.0837z^{-3} + 0.5419z^{-4} + 0.1084z^{-5}}{1 + 0.9853z^{-1} + 0.9738z^{-2} + 0.3864z^{-3} + 0.1112z^{-4} + 0.0113z^{-5}} \tag{21}$$

3.4.1 Same-Order System

Eq. (22) defines the transfer function of the fifth-order IIR system, which introduces a higher-dimensional and more complex pole–zero configuration compared to the second-order case. This increases the difficulty of the identification task due to the larger search space and stronger multimodality of the error surface. The performance comparison in Fig. 9 shows that HSFOADE achieves the lowest MSE values, tightly clustered near the global optimum with minimal variance across 25 runs. SFOA attains significantly

higher errors, while AOO and MGO converge more slowly and settle at intermediate levels. SMA again performs the weakest, displaying the most extensive spread and the highest error floor. These results confirm that HSFOADE scales effectively to higher-order systems and provides stable and accurate identification in challenging conditions

$$H_{2,same}\left(z^{-1}\right) = \frac{b_0 + b_1 z^{-1} + b_2 z^{-2} + b_3 z^{-3} + b_4 z^{-4} + b_5 z^{-5}}{1 - a_1 z^{-1} - a_2 z^{-2} - a_3 z^{-3} - a_4 z^{-4} - a_5 z^{-5}} \tag{22}$$

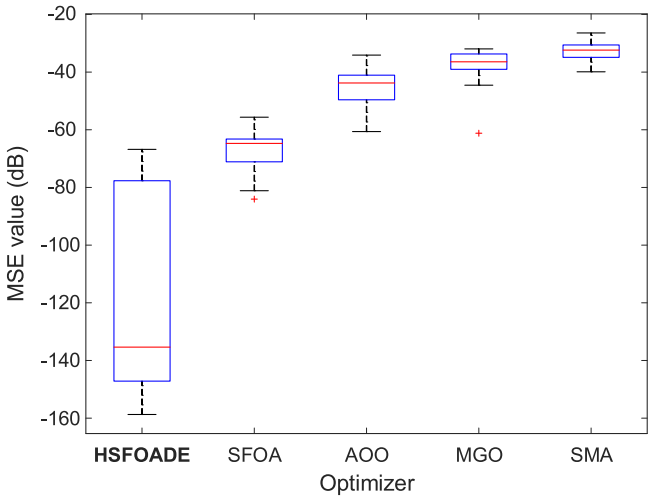

Figure 9: MSE distribution for same-order fifth-order IIR system identification using HSFOADE and baseline optimizers.

Table 8 and Fig. 10 present the results of the same-order identification for the fifth-order IIR system. HSFOADE achieves the best accuracy, with a mean MSE of 1.64×10^{-8} and a tiny standard deviation of 4.30×10^{-8}, clearly outperforming all baseline algorithms. The original SFOA yields a mean error of 3.89×10^{-7}, nearly an order of magnitude higher, while AOO and MGO converge to mean errors of 7.82×10^{-5} and 2.69×10^{-4}, respectively. SMA performs the weakest, with a mean error of 6.95×10^{-4} and the most significant variance. The convergence behaviour shown in Fig. 10 confirms these trends: HSFOADE rapidly descends toward the global optimum and stabilizes at very low error levels, whereas the competing methods stagnate at much higher error floors.

Table 8: Statistical performance of the same-order fifth-order IIR system identification across 25 runs, including nonparametric Wilcoxon signed-rank test results (p-values).

Statistical Measure	HSFOADE	SFOA	AOO	MGO	SMA
Best	1.3399E−16	3.9454E−09	8.6743E−07	7.5913E−07	1.0260E−04
Worst	2.0925E−07	2.7278E−06	3.8910E−04	6.3781E−04	2.2800E−03
Mean	1.6416E−08	3.8921E−07	7.8224E−05	2.6948E−04	6.9514E−04
SD	4.3032E−08	5.2658E−07	1.0232E−04	1.8327E−04	5.6195E−04
p-value	—	3.6243E−05	1.2290E−05	1.2290E−05	1.2290E−05

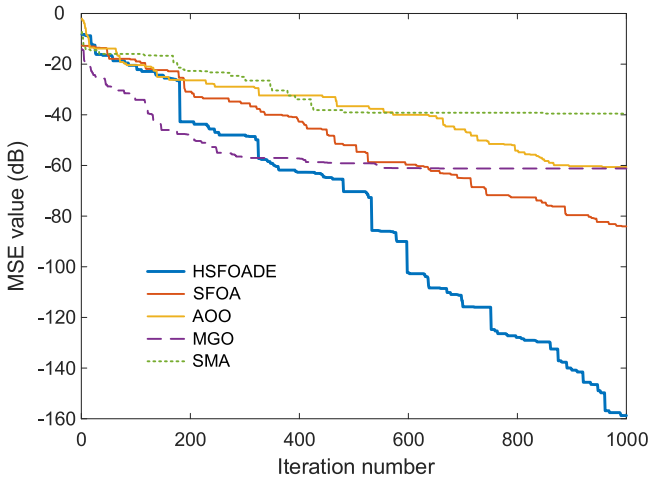

Figure 10: Convergence curves of MSE values for the same-order fifth-order IIR system identification.

Table 9 provide a detailed comparison of the coefficient estimation accuracy for the same-order fifth-order IIR system whereas Table 10 provides absolute estimation errors of the coefficients for the same-order fifth-order IIR system. HSFOADE recovers all numerator and denominator coefficients with errors on the order of 10^{-6}, confirming near-perfect reconstruction of the actual system dynamics. In contrast, SFOA shows small but noticeable deviations, with errors reaching 10^{-2} in some parameters, while AOO, MGO, and SMA produce significant mismatches, in several cases exceeding unity. These discrepancies demonstrate the difficulty of coefficient recovery in higher-order systems and emphasize HSFOADE's superiority in delivering both numerical precision and stable pole–zero placement compared to other optimizers.

Table 9: Estimated coefficients of the same-order fifth-order IIR system obtained by different optimizers.

Coefficient	Real Value	Estimated Value				
		HSFOADE	SFOA	AOO	MGO	SMA
a_1	−0.9853	−0.9853	−0.9547	0.2978	0.1231	0.0871
a_2	−0.9738	−0.9738	−0.9572	−0.2637	−0.3662	−0.0233
a_3	−0.3864	−0.3864	−0.3653	0.4798	0.3662	0.2336
a_4	−0.1112	−0.1112	−0.1087	0.0066	−0.0161	0.1700
a_5	−0.0113	−0.0113	−0.0097	0.0414	0.0385	−0.0285
b_0	0.1084	0.1084	0.1084	0.1081	0.1072	0.1004
b_1	0.5419	0.5419	0.5387	0.4019	0.4222	0.4302
b_2	1.0837	1.0837	1.0685	0.4481	0.5345	0.5191
b_3	1.0837	1.0837	1.0573	−0.0247	0.1300	0.0052
b_4	0.5419	0.5419	0.5209	−0.3362	−0.2165	−0.3620
b_5	0.1084	0.1084	0.1020	−0.1582	−0.1219	−0.1496

Table 10: Absolute estimation errors of the coefficients for the same-order fifth-order IIR system.

Coefficient	Absolute Error = |Real Value − Estimated Value|				
	HSFOADE	**SFOA**	**AOO**	**MGO**	**SMA**
a_1	4.3994E−06	3.0609E−02	1.2831E+00	1.1084E+00	1.0724E+00
a_2	2.0189E−06	1.6605E−02	7.1007E−01	6.0757E−01	9.5045E−01
a_3	2.9511E−06	2.1059E−02	8.6621E−01	7.5256E−01	6.1997E−01
a_4	1.6135E−07	2.5431E−03	1.1780E−01	9.5125E−02	2.8115E−01
a_5	2.5353E−07	1.6370E−03	5.2703E−02	4.9819E−02	1.7247E−02
b_0	2.1792E−08	1.6576E−05	2.7799E−04	1.2424E−03	7.9911E−03
b_1	4.8173E−07	3.2470E−03	1.4005E−01	1.1969E−01	1.1168E−01
b_2	2.1348E−06	1.5203E−02	6.3565E−01	5.4918E−01	5.6456E−01
b_3	3.6178E−06	2.6380E−02	1.1084E+00	9.5366E−01	1.0785E+00
b_4	2.7440E−06	2.0965E−02	8.7806E−01	7.5841E−01	9.0390E−01
b_5	7.9553E−07	6.3998E−03	2.6658E−01	2.3035E−01	2.5796E−01

3.4.2 Reduced-Order System

Eq. (23) defines the reduced-order model used to approximate the fifth-order IIR system with fewer parameters than the proper system. This intentional structural mismatch introduces unavoidable approximation error, providing a stricter test of optimizer strength. The results in Fig. 11 show that HSFOADE consistently achieves the lowest error levels, with MSE values tightly grouped around 4.18×10^{-7}. In comparison, SFOA converges to a higher mean of 3.16×10^{-6}, while AOO and MGO yield significantly larger errors on the order of 10^{-4}. SMA performs the weakest, with a mean error exceeding 10^{-3} and high variability across runs. These outcomes confirm that even under reduced-order modelling, HSFOADE maintains stable convergence and superior accuracy relative to baseline algorithms

$$H_{2,reduced}\left(z^{-1}\right) = \frac{b_0 + b_1 z^{-1} + b_2 z^{-2} + b_3 z^{-3} + b_4 z^{-4}}{1 - a_1 z^{-1} - a_2 z^{-2} - a_3 z^{-3} - a_4 z^{-4}} \tag{23}$$

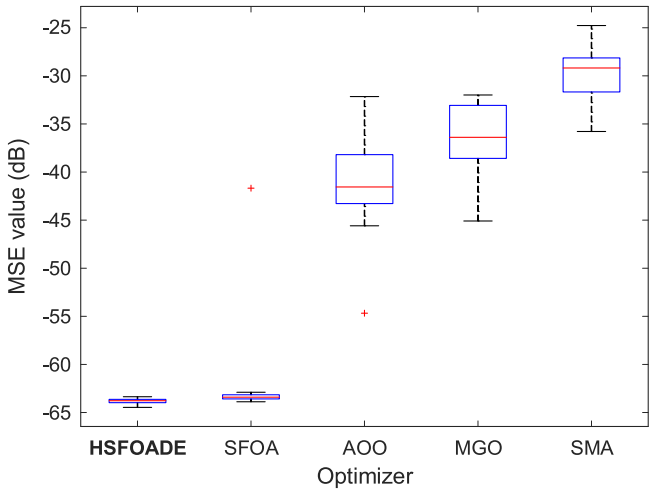

Figure 11: MSE distribution for reduced-order fifth-order IIR system identification using HSFOADE and baseline optimizers.

Table 11 and Fig. 12 summarize the results of the reduced-order identification of the fifth-order IIR system. This scenario combines model-order mismatch with high dimensionality, making it particularly challenging. HSFOADE demonstrates the strongest performance, reaching a mean MSE of 4.18×10^{-7} with a minimal standard deviation of 2.40×10^{-8}. This level of accuracy and stability is unmatched by the baseline algorithms: SFOA records a mean error of 3.16×10^{-6}, while AOO and MGO converge to values in the order of 10^{-4}, and SMA falls behind with errors above 10^{-3}. The convergence curves in Fig. 12 confirm these differences, showing HSFOADE's rapid descent to consistently low error levels compared with the slower and noisier trajectories of the other methods. These findings show that even in reduced-order, high-order identification tasks, HSFOADE stays effective, bringing precise and stable results where competing algorithms deteriorate in consistency.

Table 11: Statistical performance of reduced-order fifth-order IIR system identification across 25 runs, including nonparametric Wilcoxon signed-rank test results (p-values).

Statistical Measure	HSFOADE	SFOA	AOO	MGO	SMA
Best	3.5746E−07	4.0915E−07	3.4069E−06	3.0968E−05	2.6389E−04
Worst	4.6133E−07	6.7954E−05	6.0911E−04	6.3229E−04	3.3348E−03
Mean	4.1830E−07	3.1573E−06	1.3283E−04	2.9154E−04	1.2546E−03
SD	2.4025E−08	1.3499E−05	1.5323E−04	1.9008E−04	7.7045E−04
p-value	—	2.6647E−04	1.2290E−05	1.2290E−05	1.2290E−05

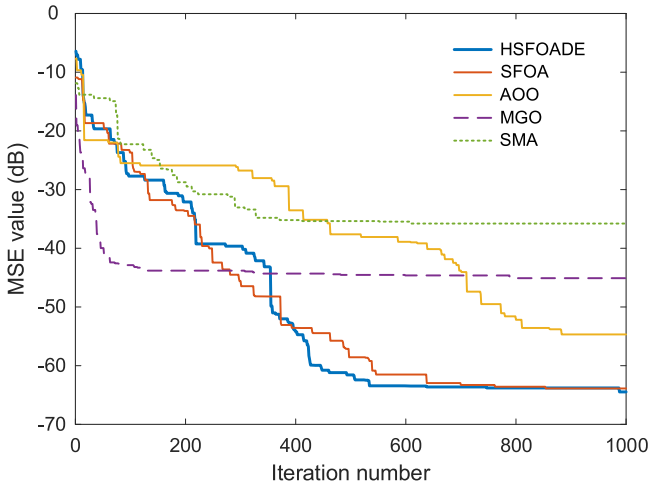

Figure 12: Convergence curves of MSE values for reduced-order fifth-order IIR system identification.

Table 12 reports the coefficient sets obtained by the different optimizers for the reduced-order fifth-order IIR model. Since the reduced-order structure differs from the original fifth-order system, a unique ground-truth coefficient vector is not defined for direct coefficient-wise comparison. Therefore, the obtained coefficients are evaluated together with the corresponding approximation errors rather than by their deviation from predefined parameter values. Among the tested methods, HSFOADE yields the lowest mean MSE and the smallest variation across independent runs, indicating the most accurate and consistent reduced-order approximation under the adopted model structure. SFOA provides the next closest performance, whereas AOO, MGO, and SMA exhibit higher approximation errors.

Table 12: Estimated coefficients of the reduced-order fifth-order IIR system obtained by different optimizers.

Coefficient	Estimated Value				
	HSFOADE	SFOA	AOO	MGO	SMA
a_1	−0.5754	−0.5899	−0.4173	0.0813	0.3061
a_2	−0.6877	−0.6912	−0.6521	−0.5364	−0.2742
a_3	−0.1000	−0.1072	−0.0230	0.2230	0.3197
a_4	−0.0441	−0.0441	−0.0516	−0.0801	−0.0308
b_0	0.1088	0.1085	0.1084	0.1062	0.1250
b_1	0.4978	0.4988	0.4814	0.4269	0.4030
b_2	0.8750	0.8808	0.8020	0.5680	0.4602
b_3	0.7033	0.7123	0.5930	0.2480	−0.0012
b_4	0.2215	0.2272	0.1542	−0.0603	−0.2920

3.4.3 Comparison with Reported Works

Table 13 focuses on the mean MSE values as the most representative metric for comparing optimizer performance in fifth-order IIR identification. In the same-order case, HSFOADE achieves the lowest mean error of 1.64×10^{-8}, clearly outperforming backtracking search algorithm (BSA) (3.43×10^{-4}) [83], PSO (7.33×10^{-2}) [83], DE (2.03×10^{-5}) [83], and average differential evolution (ADE) (2.83×10^{-6}) [83]. Even local search enhanced ADE-LS [83], which is among the strongest reported approaches with a mean of 2.73×10^{-6} remains two orders of magnitude less accurate than HSFOADE. In the reduced-order setting, HSFOADE sustains its advantage with a mean of 4.18×10^{-7}, slightly better than GOASA (4.19×10^{-7}) and clearly superior to GOA (8.27×10^{-7}), ABC (1.35×10^{-4}) [45], QPSO (4.63×10^{-3}), and HPSO-GSA (5.62×10^{-5}) [84]. These comparisons show that HSFOADE consistently delivers the lowest average error across both same-order and reduced-order cases, surpassing both classical and enhanced metaheuristics reported in the literature.

Table 13: Comparative performance of HSFOADE and reported optimizers for fifth-order IIR system identification in same- and reduced-order cases.

Type	Reference	Optimizer	MSE			
			Best	Worst	Mean	SD
Same-order	This study	HSFOADE	1.3399E−16	2.0925E−07	1.6416E−08	4.3032E−08
	[83]	BSA	2.8652E−05	0.0010	3.4336E−04	2.4050E−04
	[83]	PSO	4.6605E−06	0.3620	0.0733	0.1257
	[83]	DE	7.5274E−07	1.8014E−04	2.0264E−05	3.8949E−05
	[83]	ADE	6.3415E−08	3.2574E−05	2.8283E−06	7.8266E−06
	[83]	ADE-LS	5.1643E−15	4.0974E−05	2.7382E−06	9.4669E−06
Reduced-order	This study	HSFOADE	3.5746E−07	4.6133E−07	4.1830E−07	2.4025E−08
	[45]	GOASA	3.9165E−07	4.5756E−07	4.1907E−07	1.7476E−08
	[45]	GOA	5.2329E−07	1.3382E−06	8.2704E−07	1.8816E−07
	[45]	ABC	4.1528E−05	3.3087E−04	1.3519E−04	6.6252E−05
	[84]	QPSO	4.5405E−03	4.8683E−03	4.6331E−03	1.3374E−04
	[84]	HPSO-GSA	5.5196E−06	9.2659E−05	5.6151E−05	3.4011E−05

3.5 Validation on CEC2022 Benchmark Functions

To further examine the general optimization capability of the proposed HSFOADE algorithm, an additional benchmark validation was conducted using selected CEC2022 test functions. This experiment was included to complement the IIR system identification results and to evaluate whether the proposed hybrid search mechanism also provides consistent performance on application-independent numerical optimization problems. The selected benchmark set includes unimodal, multimodal, hybrid, and composition functions, as summarized in Table 14. All functions were evaluated in a 20-dimensional search space with lower and upper bounds of −100 and 100, respectively. The optimal function values are also reported in Table 14.

Table 14: Specifications of the CEC2022 benchmark functions.

Type	Function	Dimension	Lower Bound	Upper Bound	Optimal
Unimodal	$F_1(x)$	20	−100	100	300
	$F_2(x)$	20	−100	100	400
Multimodal	$F_3(x)$	20	−100	100	600
	$F_4(x)$	20	−100	100	800
	$F_5(x)$	20	−100	100	900
Hybrid	$F_6(x)$	20	−100	100	1800
	$F_7(x)$	20	−100	100	2000
	$F_8(x)$	20	−100	100	2200
Composition	$F_9(x)$	20	−100	100	2300
	$F_{10}(x)$	20	−100	100	2400
	$F_{11}(x)$	20	−100	100	2600
	$F_{12}(x)$	20	−100	100	2700

For this benchmark validation, HSFOADE was compared directly with its parent algorithm, SFOA. This comparison was selected to isolate the contribution of the embedded DE-based refinement mechanism within the original starfish optimization structure. Both algorithms were executed under identical experimental conditions, using 25 independent runs, a population size of 50, and 500 iterations. The performance was evaluated in terms of the best, worst, mean, and standard deviation values obtained over the independent runs.

The statistical results reported in Table 15 show that HSFOADE achieves lower mean objective values than SFOA on all selected CEC2022 functions. This indicates that the proposed hybrid mechanism provides a consistent improvement over the original SFOA across different benchmark categories. The improvement is especially visible on several multimodal and hybrid functions, where the search landscape contains many local optima and requires both population diversity and accurate local refinement. In these cases, the DE-based mutation, crossover, and greedy selection steps help guide the population toward better candidate regions while the SFOA component preserves global search capability.

In addition to lower mean values, HSFOADE generally exhibits smaller standard deviation values than SFOA, indicating more stable behaviour across independent runs. This result is important because it shows that the proposed method does not only improve the best-case performance but also reduces run-to-run variability. CEC2022 benchmark validation supports the findings obtained from the IIR identification

experiments and confirms that the proposed HSFOADE structure improves the search behaviour of SFOA in a broader numerical optimization context.

Table 15: Statistical comparison of HSFOADE and SFOA on selected CEC2022 benchmark functions.

Function	Algorithm	Best	Worst	Mean	SD
$F_1(x)$	HSFOADE	3.0404E+02	9.4092E+02	4.2750E+02	1.5971E+02
	SFOA	5.3431E+02	4.5232E+03	1.5346E+03	9.4073E+02
$F_2(x)$	HSFOADE	4.0413E+02	4.4909E+02	4.3651E+02	1.5504E+01
	SFOA	4.1351E+02	4.9950E+02	4.5700E+02	1.9162E+01
$F_3(x)$	HSFOADE	6.0000E+02	6.0004E+02	6.0001E+02	8.4786E−03
	SFOA	6.1186E+02	6.3705E+02	6.1987E+02	6.3016E+00
$F_4(x)$	HSFOADE	8.2587E+02	8.8059E+02	8.4625E+02	1.5344E+01
	SFOA	9.0732E+02	9.6577E+02	9.3980E+02	1.6888E+01
$F_5(x)$	HSFOADE	9.1493E+02	1.6701E+03	1.1371E+03	1.9694E+02
	SFOA	1.1235E+03	4.3516E+03	1.8169E+03	6.9586E+02
$F_6(x)$	HSFOADE	1.8235E+03	5.9485E+03	2.7443E+03	1.0757E+03
	SFOA	2.6723E+03	3.0138E+04	1.4742E+04	1.0064E+04
$F_7(x)$	HSFOADE	2.0053E+03	2.1010E+03	2.0356E+03	2.0095E+01
	SFOA	2.0776E+03	2.1534E+03	2.1175E+03	1.9904E+01
$F_8(x)$	HSFOADE	2.2206E+03	2.2376E+03	2.2219E+03	3.3267E+00
	SFOA	2.2358E+03	2.2568E+03	2.2429E+03	5.4734E+00
$F_9(x)$	HSFOADE	2.4808E+03	2.4808E+03	2.4808E+03	2.9926E−04
	SFOA	2.4808E+03	2.4810E+03	2.4809E+03	5.9023E−02
$F_{10}(x)$	HSFOADE	2.4202E+03	2.9541E+03	2.6095E+03	1.4688E+02
	SFOA	2.5007E+03	6.3277E+03	3.6440E+03	1.5521E+03
$F_{11}(x)$	HSFOADE	2.6000E+03	3.3111E+03	2.9567E+03	1.4654E+02
	SFOA	2.7324E+03	3.3266E+03	3.1633E+03	1.6130E+02
$F_{12}(x)$	HSFOADE	2.9344E+03	2.9587E+03	2.9463E+03	6.1759E+00
	SFOA	2.9368E+03	2.9957E+03	2.9527E+03	1.7384E+01

4 Discussion

4.1 Interpretation of the Identification Results

The results reported in Section 3 allow the behaviour of HSFOADE to be interpreted beyond the ranking of final error values. In the same-order scenarios, where an exact parametric match exists between the model and the unknown system, the true coefficient vectors of both benchmark systems were recovered by the proposed method. For the second-order system, zero absolute error was obtained for all four coefficients (Table 4), whereas for the fifth-order system the largest coefficient deviation remained on the order of 10^{-6} (Table 10). The corresponding deviations of SFOA reached the order of 10^{-2} in the denominator terms of the fifth-order model, which indicates that the parent algorithm approached the correct region of the search space but lacked the directional refinement required for its final resolution. This behaviour is consistent

with the mechanism described in Section 2.4, in which difference-based updates become dominant as the population contracts in later iterations.

A second observation concerns the relation between output error and coefficient accuracy. In the fifth-order same-order case, AOO, MGO, and SMA reached mean MSE values between 10^{-5} and 10^{-3} (Table 8), although several of their estimated denominator coefficients deviated from the true values by more than unity (Tables 9 and 10). Distinct coefficient vectors were therefore able to produce comparably small output errors, which reflects the multimodal character of the IIR error surface noted in Section 1. In such landscapes, a low MSE alone does not guarantee a faithful pole–zero description of the unknown system, and the ability of HSFOADE to attain both the lowest MSE and the correct coefficient set is regarded as a more meaningful indicator of identification quality.

In the reduced-order scenarios, the attainable error is bounded from below by the structural mismatch between the model and the reference system, and the relative differences among the algorithms are therefore necessarily smaller. For the second-order system, the mean MSE of HSFOADE (1.1692×10^{-2}) was approximately 8% lower than that of the next best method, MGO (1.2724×10^{-2}), as shown in Table 5, while for the fifth-order system its mean error (4.1830×10^{-7}) was practically identical to that reported for GOASA (4.1907×10^{-7}) in Table 13. Under these conditions, the principal advantage of the proposed method lies in its consistency rather than in large accuracy gains; the standard deviation obtained in the reduced-order fifth-order case (2.4025×10^{-8}) was more than two orders of magnitude smaller than that of SFOA (1.3499×10^{-5}), as reported in Table 11. The Wilcoxon signed-rank p-values, which remained below 3×10^{-4} in all identification scenarios (Tables 2, 5, 8 and 11), confirm that the differences with respect to the baseline optimizers are statistically significant rather than incidental.

The CEC2022 results presented in Section 3.5 indicate that these effects are not confined to the IIR identification problem. Lower mean values than those of SFOA were obtained on all twelve selected functions (Table 15), and the most pronounced improvement was observed on the hybrid function F_6, where the mean value decreased from 1.4742×10^4 to 2.7443×10^3. Standard deviations were also reduced for most functions, although the run-to-run variability of HSFOADE on F_7 remained comparable to that of SFOA. These findings suggest that the embedded refinement layer improves the search dynamics of the parent algorithm in a largely problem-independent manner, with the largest benefit on multimodal and hybrid landscapes.

4.2 Computational Cost and Practical Relevance

From a computational perspective, the asymptotic cost of HSFOADE remains of order $\mathcal{O}(NT)$ in terms of objective-function evaluations and $\mathcal{O}(NTD)$ in terms of arithmetic update operations, as analysed in Section 2.5. The DE mutation, crossover, and greedy replacement steps add only a fixed number of vector operations per individual and therefore do not alter this asymptotic order. Moreover, the convergence curves in Figs. 6, 8, 10 and 12 show that HSFOADE reaches low error levels within fewer iterations than the compared methods, which reduces the practical cost of attaining a prescribed identification accuracy.

IIR filters are critical in engineering because they can represent system dynamics compactly while achieving high accuracy with relatively low order. Their applications extend across control and automation, audio and communication systems, biomedical signal processing, and embedded real-time implementations. HSFOADE directly addresses the nonlinear error surfaces that make IIR identification challenging, ensuring accurate pole–zero recovery and stable model estimation, which makes the method suitable for these practical domains. The differences between SFOA and HSFOADE are summarized in Table 16, which highlights their mechanisms, complexity, and observed performance. This head-to-head comparison shown in following table clearly summarizes the advantage of the hybrid design over the original starfish framework.

Table 16: Head-to-head comparison of SFOA and HSFOADE in IIR identification.

Aspect	SFOA	HSFOADE (Proposed)
Core mechanism	Exploration, preying, regeneration	SFOA structure + DE mutation/ crossover + greedy selection
Oracle complexity	$\mathcal{O}(NT)$	$\mathcal{O}(NT) + (DEop.)$
Empirical convergence	Slower descent, higher residuals	Faster descent, lower residuals
Accuracy in higher-order IIR	Moderate, sensitive to local minima	High, stable coefficients and lower MSE
Literature benchmark	Below advanced metaheuristics	Outperforms strong methods (ADE-LS, GOASA, etc.)

The improvement achieved by HSFOADE is not solely due to hybridization but arises from the complementary interaction between stochastic exploration and difference-based directional refinement. This interaction enables more stable convergence and reduces parameter estimation variance, particularly in the denominator coefficients that govern system stability.

4.3 Limitations of the Study

Although the obtained results confirm the effectiveness of HSFOADE for IIR system identification, several limitations should be acknowledged. First, the experimental validation is based on a limited number of benchmark IIR systems, including second-order and fifth-order cases. Therefore, the conclusions should be interpreted within the scope of these controlled identification scenarios. Second, the study mainly relies on synthetic reference systems with known coefficients, which enables fair quantitative comparison but does not fully represent all uncertainties encountered in real signal acquisition environments. Third, although the same-order and reduced-order cases provide useful evidence of accuracy and model compactness, broader filter structures, higher-order systems, and real signal processing datasets were not considered in the present evaluation. In addition, the DE control parameters were kept fixed (F = 0.5 and CR = 0.7) in order to isolate the effect of the hybrid structure, and stability of the estimated models was not imposed as an explicit constraint in Eq. (16); instead, the search was confined to the coefficient bounds given in Section 3.2 and guided by the output error.

5 Conclusion and Future Work

This study presented HSFOADE, a hybrid starfish–differential evolution algorithm in which DE mutation, crossover, and greedy selection are embedded as a refinement layer within each SFOA iteration, and applied it to the identification of IIR systems under both same-order and reduced-order conditions. Across the second- and fifth-order benchmark systems, lower mean MSE values and smaller run-to-run variability were obtained than with the original SFOA and the AOO, MGO, and SMA baselines, and the true coefficient vectors were recovered in the same-order cases. The results were also better than, or comparable to, those reported for strong literature methods such as ADE-LS and GOASA, and consistent improvements over SFOA were observed on the selected CEC2022 benchmark functions. Based on these findings, the main contributions of this study are summarized below:

- A new hybrid optimization algorithm, HSFOADE, that embeds DE operators within the SFOA framework, enhancing variation and selection.
- Same asymptotic complexity as SFOA, but with improved practical efficiency through faster convergence.
- Enhanced performance in IIR identification across second and fifth-order, same- and reduced-order cases.
- Accurate parameter estimation with reliable pole–zero recovery, which is critical for system stability.
- Clear advantage over both baseline algorithms and advanced optimizers reported in the literature.
- Application potential in control, audio/communications, biomedical signal processing, and real-time embedded systems, where compact and accurate IIR models are essential.
- A comprehensive comparative evaluation is established, including same-order and reduced-order identification scenarios, convergence analysis, and statistical performance indicators, providing a consistent basis for assessing the behaviour of the proposed method against representative optimization algorithms.

Several directions are envisaged for future work. First, the evaluation will be extended to a wider set of benchmark filters, including higher-order systems and alternative realizations such as lattice and parallel structures, together with real signal processing datasets acquired under practical measurement conditions. Second, the robustness of HSFOADE will be examined when the desired output is corrupted by measurement noise, as commonly encountered in adaptive identification settings. Third, self-adaptive schemes for the scaling factor F and crossover rate CR, which were fixed in the present study, will be investigated together with explicit stability-handling mechanisms for the denominator coefficients. Finally, the low arithmetic overhead of the method motivates its implementation on embedded and FPGA-based platforms [56–58], where compact and accurate IIR models are required for real-time operation.

Acknowledgement: Generative AI tools were used only for language editing during manuscript revision. All technical content and final revisions were reviewed and approved by the authors.

Funding Statement: The authors received no specific funding for this study.

Author Contributions: Serdar Ekinci, Ridvan Firat Cinar, Davut Izci, Gökhan Yüksek: Conceptualization, Methodology, Software, Visualization, Investigation, Writing—Original Draft Preparation. Vedat Tümen, Timur Lale, Behçet Kocaman, Filiz Karaomerlioglu, Fahmi Elsayed, Mohammad Salman: Data Curation, Validation, Supervision, Writing—Review & Editing. All authors reviewed and approved the final version of the manuscript.

Availability of Data and Materials: All data supporting the findings of this study are presented within the manuscript.

Ethics Approval: Not applicable. This study does not involve human participants, animals, or identifiable personal data.

Conflicts of Interest: The authors declare no conflicts of interest.

References

1. Oppenheim AV, Willsky AS, Nawab SH. Signals and systems. 2nd ed. Upper Saddle River, NJ, USA: Prentice Hall; 1997. 957 p.
2. Proakis JG, Manolakis DG. Digital signal processing: principles, algorithms and applications. 5th ed. Harlow, UK: Pearson Education; 2021. 1146 p.
3. Vaseghi SV. Advanced digital signal processing and noise reduction. New York, NY, USA: J. Wiley & Sons; 2008. 514 p. doi:10.1002/9780470740156.

4. Stamatopoulos I, Koutzoglou I, Karatzidis DI, Zaharis ZD, Lazaridis PI, Kantartzis NV. Efficient filter design to compensate fabrication imperfections in 6G communication systems. Sensors. 2023;23(24):9825. doi:10.3390/s23249825.
5. Srinivasagan R. Advanced low-power filter architecture for biomedical signals with adaptive tuning. PLoS One. 2025;20(1):e0311768. doi:10.1371/journal.pone.0311768.
6. Asgari S, Mehrnia A. A novel low-complexity digital filter design for wearable ECG devices. PLoS One. 2017;12(4):e0175139. doi:10.1371/journal.pone.0175139.
7. Razee AM, Dziyauddin RA, Azmi MH, Sadon SK. Comparative performance analysis of IIR and FIR filters for 5G networks. In: Proceedings of the 2018 2nd International Conference on Telematics and Future Generation Networks (TAFGEN); 2018 Jul 24–26; Kuching, Malaysia. p. 143–8. doi:10.1109/TAFGEN.2018.8580470.
8. Cuevas E, Avalos O, Gálvez J. IIR system identification using several optimization techniques: a review analysis. In: Analysis and comparison of metaheuristics. Cham, Switzerland: Springer; 2023. p. 89–104. doi:10.1007/978-3-031-20105-9_5.
9. Regalia PA. Adaptive IIR filtering in signal processing and control. Oxfordshire, UK: Routledge; 2018. doi:10.1201/9781315136653.
10. Oppenheim AV, Schafer RW. Filter design techniques. In: Discrete-time signal processing. 3rd ed. Upper Saddle River, NJ, USA: Pearson; 2010. p. 493–622.
11. Välimäki V, Reiss JD. All about audio equalization: solutions and frontiers. Appl Sci. 2016;6(5):129. doi:10.3390/app6050129.
12. Pepe G, Gabrielli L, Squartini S, Tripodi C, Strozzi N. Deep optimization of parametric IIR filters for audio equalization. IEEE/ACM Trans Audio Speech Lang Process. 2022;30(11):1136–49. doi:10.1109/TASLP.2022.3155289.
13. Karuppaiah R, Seerengasamy U, Boobalakrishnan N. Enhanced digital acoustic perception in hearing aid device using reconfigurable filter bank structure: a systematic review with recommendation. Audit Vestib Res. 2025. doi:10.18502/avr.v34i2.18052.
14. Patole SM, Torlak M, Wang D, Ali M. Automotive radars: a review of signal processing techniques. IEEE Signal Process Mag. 2017;34(2):22–35. doi:10.1109/MSP.2016.2628914.
15. Middlestead RW. Digital communications with emphasis on data modems: theory, analysis, design, simulation, testing, and applications. New York, NY, USA: Wiley; 2017. 792 p. doi:10.1002/9781119011866.
16. Sutradhar SR, Sayadat N, Rahman A, Munira S, Haque AKMF, Sakib SN. IIR based digital filter design and performance analysis. In: Proceedings of the 2017 2nd International Conference on Telecommunication and Networks (TEL-NET); 2017 Aug 10–11; Noida, India. p. 1–6. doi:10.1109/TEL-NET.2017.8343596.
17. Krukowski A, Kale İ. DSP system design. Boston, MA, USA: Springer US; 2003. 234 p. doi:10.1007/b105738.
18. Singh R, Arya SK. Genetic algorithm for the design of optimal IIR digital filters. J Signal Inf Process. 2012;3(3):286–92. doi:10.4236/jsip.2012.33038.
19. Krusienski DJ, Jenkins WK. Particle swarm optimization for adaptive IIR filter structures. In: Proceedings of the 2004 Congress on Evolutionary Computation; 2004 Jun 19–23; Portland, OR, USA. p. 965–70. doi:10.1109/CEC.2004.1330966.
20. Su TJ, Zhuang QY, Lin WH, Hung YC, Yang WR, Wang SM. Design of infinite impulse response filters based on multi-objective particle swarm optimization. Signals. 2024;5(3):526–41. doi:10.3390/signals5030029.
21. Storn R. Differential evolution design of an IIR-filter. In: Proceedings of IEEE International Conference on Evolutionary Computation; 1996 May 20–22; Nagoya, Japan. p. 268–73. doi:10.1109/ICEC.1996.542373.
22. Karaboga N. Digital IIR filter design using differential evolution algorithm. EURASIP J Adv Signal Process. 2005;2005(8):856824. doi:10.1155/ASP.2005.1269.
23. Mirjalili S, Mirjalili SM, Lewis A. Grey wolf optimizer. Adv Eng Softw. 2014;69:46–61. doi:10.1016/j.advengsoft.2013.12.007.
24. Karaboga N. A new design method based on artificial bee colony algorithm for digital IIR filters. J Frankl Inst. 2009;346(4):328–48. doi:10.1016/j.jfranklin.2008.11.003.

25. Singh S, Ashok A, Kumar M, Garima, Rawat TK. Optimal design of IIR filter using dragonfly algorithm. In: Applications of artificial intelligence techniques in engineering. Singapore: Springer; 2019. p. 211–23. doi:10.1007/978-981-13-1819-1_21.
26. Dash J, Dam B, Swain R. Improved firefly algorithm based optimal design of special signal blocking IIR filters. Measurement. 2020;149(4):106986. doi:10.1016/j.measurement.2019.106986.
27. Liu A, Li P, Deng X, Ren L. A sigmoid attractiveness based improved firefly algorithm and its applications in IIR filter design. Connect Sci. 2021;33(1):1–25. doi:10.1080/09540091.2020.1742660.
28. Panda G, Pradhan PM, Majhi B. IIR system identification using cat swarm optimization. Expert Syst Appl. 2011;38(10):12671–83. doi:10.1016/j.eswa.2011.04.054.
29. Cinar RF. Enzyme action optimizer based infinite impulse response filter identification through a comprehensive benchmark across full and reduced orders. Sci Rep. 2025;15(1):44577. doi:10.1038/s41598-025-28411-w.
30. Rodan A, Al-Tamimi AK, Al-Alnemer L, Mirjalili S, Tiňo P. Enzyme action optimizer: a novel bio-inspired optimization algorithm. J Supercomput. 2025;81(5):686. doi:10.1007/s11227-025-07052-w.
31. Amiri MH, Mehrabi Hashjin N, Montazeri M, Mirjalili S, Khodadadi N. Hippopotamus optimization algorithm: a novel nature-inspired optimization algorithm. Sci Rep. 2024;14(1):5032. doi:10.1038/s41598-024-54910-3.
32. Ekinci S, Izci D, Yilmaz M. Simulated annealing aided artificial hummingbird optimizer for infinite impulse response system identification. IEEE Access. 2023;11:88627–36. doi:10.1109/ACCESS.2023.3303328.
33. Ekinci S, Izci D, Kayri M. Artificial hummingbird optimizer as a novel adaptive algorithm for identifying optimal coefficients of digital IIR filtering systems. Int J Model Simul. 2025;45(3):838–52. doi:10.1080/02286203.2023.2240564.
34. Rizk-Allah RM, Ekinci S, Izci D. An improved artificial rabbits optimization for accurate and efficient infinite impulse response system identification. Decis Anal J. 2023;9:100355. doi:10.1016/j.dajour.2023.100355.
35. Dalirinia E, Jalali M, Yaghoobi M, Tabatabaee H. Lotus effect optimization algorithm (LEA): a lotus nature-inspired algorithm for engineering design optimization. J Supercomput. 2024;80(1):761–99. doi:10.1007/s11227-023-05513-8.
36. Jalali M, Vu B, Chandna S, Nadimi-Shahraki MH. SOCIAL: social network optimization algorithm via centrality and influence-aware learning. Appl Soft Comput. 2026;194(4):114914. doi:10.1016/j.asoc.2026.114914.
37. Zhong C, Li G, Meng Z, Li H, Yildiz AR, Mirjalili S. Starfish optimization algorithm (SFOA): a bio-inspired metaheuristic algorithm for global optimization compared with 100 optimizers. Neural Comput Appl. 2025;37(5):3641–83. doi:10.1007/s00521-024-10694-1.
38. Saha SK, Kar R, Mandal D, Ghoshal SP. Gravitation search algorithm: application to the optimal IIR filter design. J King Saud Univ Eng Sci. 2014;26(1):69–81. doi:10.1016/j.jksues.2012.12.003.
39. Zhao S, Li Z, Yun X, Wang K, Lyu X, Liu B. IIR filters designing by water wave optimization. In: Proceedings of the 2017 13th IEEE International Conference on Control & Automation (ICCA); 2017 Jul 3–6; Ohrid, Macedonia. p. 347–52. doi:10.1109/ICCA.2017.8003085.
40. Mohammadi A, Sheikholeslam F, Mirjalili S. Inclined planes system optimization: theory, literature review, and state-of-the-art versions for IIR system identification. Expert Syst Appl. 2022;200(3):117127. doi:10.1016/j.eswa.2022.117127.
41. Lagos-Eulogio P, Seck-Tuoh-Mora JC, Hernandez-Romero N, Medina-Marin J. A new design method for adaptive IIR system identification using hybrid CPSO and DE. Nonlinear Dyn. 2017;88(4):2371–89. doi:10.1007/s11071-017-3383-7.
42. Dai C, Chen W, Zhu Y. Seeker optimization algorithm for digital IIR filter design. IEEE Trans Ind Electron. 2010;57(5):1710–8. doi:10.1109/TIE.2009.2031194.
43. Wang Y, Li B, Weise T. Two-stage ensemble memetic algorithm: function optimization and digital IIR filter design. Inf Sci. 2013;220(2):408–24. doi:10.1016/j.ins.2012.07.041.
44. Mittal T. A hybrid moth flame optimization and variable neighbourhood search technique for optimal design of IIR filters. Neural Comput Appl. 2022;34(1):689–704. doi:10.1007/s00521-021-06379-8.
45. Ekinci S, Izci D. Enhancing IIR system identification: harnessing the synergy of gazelle optimization and simulated annealing algorithms. e-Prime Adv Electr Eng Electron Energy. 2023;5:100225. doi:10.1016/j.prime.2023.100225.

46. Tsai JT, Chou JH. Design of optimal digital IIR filters by using an improved immune algorithm. IEEE Trans Signal Process. 2006;54(12):4582–96. doi:10.1109/TSP.2006.881248.
47. Singh R, Verma HK. Teaching–learning-based optimization algorithm for parameter identification in the design of IIR filters. J Inst Eng India Ser B. 2013;94(4):285–94. doi:10.1007/s40031-013-0063-y.
48. Dewangan S, Yadav S, Saha SK. IIR filter design using sparrow search algorithm. In: Proceedings of the 2024 15th International Conference on Computing Communication and Networking Technologies (ICCCNT); 2024 Jun 24–28; Kamand, India. p. 1–6. doi:10.1109/ICCCNT61001.2024.10725733.
49. Ekinci S, Izci D, Eker E, Abualigah L, Thanh CL, Khatir S. Hunger games pattern search with elite opposite-based solution for solving complex engineering design problems. Evol Syst. 2024;15(3):939–64. doi:10.1007/s12530-023-09526-9.
50. Ekinci S, İzci D. Pattern search ameliorated arithmetic optimization algorithm for engineering optimization and infinite impulse response system identification. ELECTRICA. 2024;24(1):119–30. doi:10.5152/electrica.2023.22234.
51. Agrawal N, Kumar A, Bajaj V. Optimized design of digital IIR filter using artificial bee colony algorithm. In: Proceedings of the 2015 International Conference on Signal Processing, Computing and Control (ISPCC); 2015 Sep 24–26; Waknaghat, India. p. 316–21. doi:10.1109/ISPCC.2015.7375048.
52. Ersalı C, Hekimoğlu B. Improved cooperation search optimization algorithm for infinite impulse response system identification. ELECTRICA. 2024;24(3):733–47. doi:10.5152/electrica.2024.24075.
53. Mohammadi A, Zahiri SH, Razavi SM, Suganthan PN. Design and modeling of adaptive IIR filtering systems using a weighted sum–variable length particle swarm optimization. Appl Soft Comput. 2021;109(4):107529. doi:10.1016/j.asoc.2021.107529.
54. Sharma S, Kumar S, Nayyar A. Logarithmic spiral based local search in artificial bee colony algorithm. In: Industrial networks and intelligent systems. Cham, Switzerland: Springer; 2019. p. 15–27. doi:10.1007/978-3-030-05873-9_2.
55. Chen L, Liu M, Wang Z, Dai Z. A structure evolution-based design for stable IIR digital filters using AMECoDEs algorithm. Soft Comput. 2020;24(7):5151–63. doi:10.1007/s00500-019-04268-w.
56. Mondal S, Sarkar S, Aich RM, Dhabal S, Venkateswaran P. An improved IIR filter design using artificial rabbits optimization algorithm and its FPGA implementation. In: Proceedings of the 2025 Devices for Integrated Circuit (DevIC); 2025 Apr 5–6; Kalyani, India. p. 670–5. doi:10.1109/devic63749.2025.11012617.
57. Pandey A, Pratibha E. A review of techniques for optimization and implementation of digital filters on FPGA. Int J Res Appl Sci Eng Technol. 2022;10(6):1133–9. doi:10.22214/ijraset.2022.43516.
58. Abdullah SA, Hamad AA. FPGA-based digital filter design: a review paper. In: Proceedings of the 2024 3rd International Conference on Advances in Engineering Science and Technology (AEST); 2024 Nov 24–25; Babil, Iraq. p. 102–7. doi:10.1109/AEST63017.2024.10960160.
59. Mahata S, Herencsar N, Baykant Alagoz B, Yeroglu C. Reduced order infinite impulse response system identification using manta ray foraging optimization. Alex Eng J. 2024;87(3):448–77. doi:10.1016/j.aej.2023.12.054.
60. Dey S, Roy PK, Chakraborty S. Optimal design of IIR-type fractional order digital integrator using mayfly optimization algorithm. Circuits Syst Signal Process. 2023;42(2):913–42. doi:10.1007/s00034-022-02141-0.
61. Mohammadi A, Zahiri SH, Razavi SM. Infinite impulse response systems modeling by artificial intelligent optimization methods. Evol Syst. 2019;10(2):221–37. doi:10.1007/s12530-018-9218-z.
62. Abualigah L, Izci D, Jabari M, Ekinci S, Saleem K, Migdady H, et al. Adaptive gbest-guided atom search optimization for designing stable digital IIR filters. Circuits Syst Signal Process. 2025;44(6):4059–81. doi:10.1007/s00034-025-02997-y.
63. Ekinci S, Budak C, Izci D, Gider V. An atom search optimization approach for IIR system identification. Int J Model Simul. 2025;45(4):1448–64. doi:10.1080/02286203.2023.2287968.
64. Dey S, Roy PK, Sarkar A. Adaptive IIR model identification using chaotic opposition-based whale optimization algorithm. J Electr Syst Inf Technol. 2023;10(1):33. doi:10.1186/s43067-023-00102-4.
65. Niu Y, Yan X, Wang Y, Niu Y. Dynamic opposite learning enhanced artificial ecosystem optimizer for IIR system identification. J Supercomput. 2022;78(11):13040–85. doi:10.1007/s11227-022-04367-w.
66. Yang Y, Yang B, Niu M. Adaptive infinite impulse response system identification using opposition based hybrid coral reefs optimization algorithm. Appl Intell. 2018;48(7):1689–706. doi:10.1007/s10489-017-1034-9.

67. Zhong C, Chen H, Xin D, Xu T, Meng Z, Wang X, et al. Opposition and reinforcement learning growth-starfish optimization algorithm for engineering design and feature selection. Knowl Based Syst. 2026;338(1):115522. doi:10.1016/j.knosys.2026.115522.
68. Chen H, Xu T, Huang Y, Xin D, Zhong C. MCPSFOA: multi-strategy enhanced crested porcupine-starfish optimization algorithm for global optimization and engineering design. Comput Model Eng Sci. 2026;146(1):16–10. doi:10.32604/cmes.2026.075792.
69. Shynk JJ. Adaptive IIR filtering. IEEE ASSP Mag. 1989;6(2):4–21. doi:10.1109/53.29644.
70. Ljung L. System identification: theory for the user. 2nd ed. Upper Saddle River, NJ, USA: Prentice Hall PTR; 1999.
71. Izci D, Ekinci S, Hussien AG. An elite approach to re-design Aquila optimizer for efficient AFR system control. PLoS One. 2023;18(9):e0291788. doi:10.1371/journal.pone.0291788.
72. Izci D, Hashim FA, Mostafa RR, Ekinci S, Smerat A, Migdady H, et al. Efficient optimization of engineering problems with a particular focus on high-order IIR modeling for system identification using modified dandelion optimizer. Optim Control Appl Methods. 2025;46(4):1470–510. doi:10.1002/oca.3274.
73. Ekinci S, Izci D, Al Nasar MR, Abu Zitar R, Abualigah L. Logarithmic spiral search based arithmetic optimization algorithm with selective mechanism and its application to functional electrical stimulation system control. Soft Comput. 2022;26(22):12257–69. doi:10.1007/s00500-022-07068-x.
74. Pan J, Tompkins WJ. A real-time QRS detection algorithm. IEEE Trans Biomed Eng. 1985;BME-32(3):230–6. doi:10.1109/TBME.1985.325532.
75. Rämö J, Välimäki V, Bank B. High-precision parallel graphic equalizer. IEEE/ACM Trans Audio Speech Lang Process. 2014;22(12):1894–904. doi:10.1109/TASLP.2014.2354241.
76. Karmakar P, Dhar S, Chakraborty M, Paul T. Comparative study of four different types of MTI filters for radar clutter rejection. Int J Image Graph Signal Process. 2013;5(5):40–6. doi:10.5815/ijigsp.2013.05.05.
77. Storn R, Price K. Differential evolution—a simple and efficient heuristic for global optimization over continuous spaces. J Glob Optim. 1997;11(4):341–59. doi:10.1023/A:1008202821328.
78. Maiti B, Biswas S, Ezugwu AES, Bera UK, Alzahrani AI, Alblehai F, et al. Enhanced crayfish optimization algorithm with differential evolution's mutation and crossover strategies for global optimization and engineering applications. Artif Intell Rev. 2025;58(3):69. doi:10.1007/s10462-024-11069-7.
79. Ramalakshmi K, Shiney JRJ, Kumari LK, Rajalakshmi R. Analysis of nonlinear optimization problems using differential evolution algorithm. In: Women in soft computing. Cham, Switzerland: Springer; 2024. p. 21–46. doi:10.1007/978-3-031-44706-8_2.
80. Wang RB, Hu RB, Geng FD, Xu L, Chu SC, Pan JS, et al. The animated oat optimization algorithm: a nature-inspired metaheuristic for engineering optimization and a case study on wireless sensor networks. Knowl Based Syst. 2025;318:113589. doi:10.1016/j.knosys.2025.113589.
81. Abdollahzadeh B, Gharehchopogh FS, Khodadadi N, Mirjalili S. Mountain gazelle optimizer: a new nature-inspired metaheuristic algorithm for global optimization problems. Adv Eng Softw. 2022;174(3):103282. doi:10.1016/j.advengsoft.2022.103282.
82. Li S, Chen H, Wang M, Heidari AA, Mirjalili S. Slime mould algorithm: a new method for stochastic optimization. Future Gener Comput Syst. 2020;111:300–23. doi:10.1016/j.future.2020.03.055.
83. Durmuş B. Infinite impulse response system identification using average differential evolution algorithm with local search. Neural Comput Appl. 2022;34(1):375–90. doi:10.1007/s00521-021-06399-4.
84. Jiang S, Wang Y, Ji Z. A new design method for adaptive IIR system identification using hybrid particle swarm optimization and gravitational search algorithm. Nonlinear Dyn. 2015;79(4):2553–76. doi:10.1007/s11071-014-1832-0.